TERMOFLUIDODINAMICA COMPUTAZIONALE: INTRODUZIONE

Enrico Nobile

Dipartimento di Ingegneria e Architettura
Università degli Studi di Trieste, 34127 TRIESTE

12 marzo 2024

OUTLINE

Parte I

Overview

1. Cos'è la CFD (TCFD)
2. Ambiti applicativi della CFD
3. Limiti e potenzialità delle tecniche CFD

La CFD (TCFD)

Cos'è la Termofluidodinamica (o Fluidodinamica) Computazionale ?

- TCFD – Termofluidodinamica Computazionale = CFD – Computational Fluid Dynamics + NHT – Numerical Heat Transfer;
- Con CFD intendiamo l'insieme delle tecniche, numeriche e non, utilizzate per la soluzione (previsione) approssimata del moto dei fluidi e dei fenomeni associati (scambio termico, scambio di materia, combustione, reazioni chimiche etc.);
- Con le tecniche CFD, la soluzione delle equazioni differenziali (o integro-differenziali) che governano i fenomeni (continuità, quantità di moto, energia, etc.), è approssimata attraverso la discretizzazione del dominio - spaziale e temporale) - di interesse:
  - Il problema da continuo diviene discreto;
  - La CFD è profondamente legata all'esistenza ed utilizzo del computer.

La CFD (TCFD) - *cont.*

- CFD can provide information on:
  - Distribution of velocity, pressure, temperatute et.
  - Forces (Lift, Drag);
  - Distribution of multiples phases (gas-liquid, gas-solid et.);
  - More...
- CFD and NHT can be used in different stages of the engineering process:
  - Initial conceptual (exploratory) studies;
  - Detailed product development;
  - Optimization;
  - Troubleshooting & redesign.
- CFD complements experimentation (at real-scale or model-scale) reducing overall costs, time, number of experimental prototypes et.

CFD vs NFD

- Qualcuno (Roache, 1976) distingue fra *Computational Fluid Dynamics* (o, in modo equivalente, *Numerical Simulation of Fluid Dynamics*) dal termine più generale *Numerical Fluid Dynamics*;
- Con *Numerical Fluid Dynamics* si intendono tutte le tecniche numeriche applicate alla soluzione di problemi fluidodinamici (Equazioni differenziali ordinarie, metodo delle caratteristiche etc.);
- Con CFD, inoltre, si intendono, oltre alle applicazioni tipiche in ambito industriale, anche le attività di ricerca ad essa associate (di base, applicata e pre-competitiva) indirizzate ai metodi (es. metodi numerici), ai modelli (es. turbolenza, combustione etc.) ed alle applicazioni.

CFD: materia multidisciplinare

Panoramica delle discipline *contenute* nella CFD:

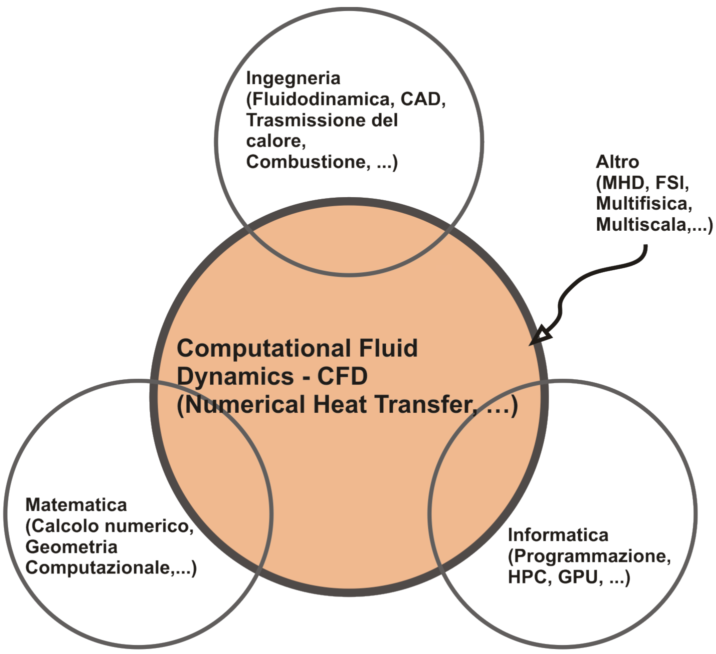

Cenni storici

- La CFD è nata originariamente all'interno dei grandi centri di ricerca, pubblici e privati, attorno agli anni '60 [Los Alamos: J. Von Neumann, 1950; Harlow and Welch (Physics of Fluids), 1965. IBM: Fromm J.E. (IBM J. Research and Development), 1971];
- Inizialmente si è diffusa quasi esclusivamente in ambito aeronautico ed aerospaziale (in-house codes);
- Successivamente, grazie al continuo incremento delle prestazioni delle piattaforme di calcolo ed alla riduzione dei relativi costi, ed allo sviluppo di pacchetti CFD commerciali, si è via via diffusa in ambito Accademico ed in alcuni settori industriali (automotive, turbomacchine, energia etc.);
- Attualmente il suo utilizzo è sempre più diffuso, a seguito di:
  - Disponibilità di pacchetti CFD commerciali (industriali) sempre più versatili e ricchi di funzionalità (modelli, facilità d'uso, integrazione CAD etc.);
  - Disponibilità di librerie e pacchetti Open Source;
  - Hardware dalle prestazioni crescenti e dai costi ridotti (multi-core, clusters, GPUs etc.).
- I campi applicativi della CFD sono numerosissimi, e riguardano qualunque disciplina e/o problema in cui il moto dei fluidi rivesta un certo interesse;
- Possiamo elencarli (1) per settore applicativo e (2) per applicazione.

Settori applicativi

Un possibile elenco - non esaustivo - è il seguente:

- Ricerca di base ed applicata;
- Attività formativa;
- Settore aeronautico ed aerospaziale;
- Settore automobilistico;
- Settore navale ed off-shore;
- Settore ferroviario;
- Ingegneria elettrica ed elettronica;
- Bioingegneria e medicale;
- Industria chimica e di processo;
- Nanotecnologie;
- Ingegneria Civile ed Ambientale;
- Settore energetico (tradizionale, fonti rinnovabili, nucleare, fusione etc.);
- Sport (Automobilistico, motociclistico, sailing, ciclismo, sci, nuoto etc.);
- Sicurezza (esplosioni, incendi etc.).

Applicazioni

Le possibili applicazioni sono numerosissime, vediamone alcune:

- Aerodinamica esterna (velivoli, automobili, treni etc.);
- Idrodinamica con superficie libera (navi, imbarcazioni);
- Fluidodinamica e combustione di motori a combustione interna;
- Turbomacchine (pompe, compressori, turbine idrauliche, turbine a vapore ed a gas, generatori eolici);
- Scambio termico (scambiatori di calore, controllo termico in microelettronica);
- Magnetofluidodinamica (freni e *stirrer* elettromagnetici nei processi di produzione e colata continua di metalli);
- Propulsori navali, in presenza o meno di cavitazione.

Nel seguito, illustriamo alcune di queste svolte presso il gruppo di *Fisica Tecnica* del Dipartimento di Ingegneria e Architettura (DIA), o in altri enti/società nell'ambito di collaborazioni e progetti di ricerca comuni.

Vantaggi e svantaggi

Metodo	Vantaggi	Svantaggi
Sperimentale	• Maggiormente realistico	• Necessità di attrezzature e strumentazione; • Problemi di scala; • Difficoltà di misura - perturbazioni; • Costi operativi.
Analitico	• Informazione semplice, spesso in forma "chiusa", di uso generale.	• Limitato a geometria e fisica *semplici*; • Usualmente limitato a problemi lineari.
CFD	• Non limitato a problemi lineari; • Fisica e geometria *complesse*; • Problemi stazionari e non stazionari; • Costi in progressiva diminuzione; • Buona e/o ottima integrazione nel processo progettuale.	• Errori di discretizzazione e di modellazione; • Difficoltà nelle condizioni al contorno; • Semplificazioni; • Difficoltà di interpretazione.

CFD - e la *simulazione* in generale - costituiscono un fattore fondamentale per incrementare il tasso di *innovazione* di prodotti e servizi.

Aspetti peculiari della CFD

La CFD è più vicina all'analisi sperimentale, che all'approccio teorico, visti i limiti attuali della teoria matematica delle equazioni alle derivate parziali:

- Stabilità;
- Stima dell'errore;
- Convergenza.

In qualche caso, fenomeni sono stati scoperti prima per via numerica (es. Campbell e Mueller 1968: subsonic ramp-induced separation [1]), ed in altri casi (rari) la simulazione numerica ha smentito rilievi sperimentali affetti da errori sistematici (es. Stalio e Nobile 2003: heat transfer over riblets [2]).

In CFD, ed in particolare per applicazioni industriali, è spesso necessario basarsi sull'analisi matematica di problemi semplificati, basati sull'ipotesi di linearità, ma soprattutto su ragionamenti euristici, intuito, esperienza ed approcci *trial and error*.

[1] Campbell, D. R., Mueller, T. J., A Numerical and Experimental Investigation of Incompressible Laminar-Induced Separated Flow, University of Notre Dame, Department of Aerospace Engineering, *Report UNDAS TN-1068-M1*,(1968).

[2] Stalio, E., Nobile, E., Direct numerical simulation of heat transfer over riblets, *Int. J. Heat and Fluid Flow*, **24**, pp. 356-371, (2003).

CFD *Vs* Metodo Sperimentale

Le tecniche CFD non sono (e non lo saranno per molto tempo) completamente sostitutive dell'approccio sperimentale:

- Le equazioni (continue) costitutive non possono, a rigore, definirsi esatte;
- Il processo di discretizzazione - l'analogia perfetta fra equazioni continue e discretizzate vale solo per dimensione di griglia nulla - può alterare anche il comportamento qualitativo delle equazioni (es. diffusività artificiale);
- Fenomeni su scala molto *piccola* possono essere solo approssimati (es. turbolenza, combustione etc.).

OUTLINE

Parte II

Historical notes

The beginning...

- CFD (Computational Fluid Dynamics) and CHT (Computational Heat Transfer):
  - Term *CFD* invented by C.K. Chu of Columbia University.
  - It gained popularity with P. Roache, *Computational fluid dynamics*, 1972.
- Los Alamos WWII Manhattan Project:
  - H. Bethe and R. Feynman computed the energy released for the plutonium bomb.
  - Feynman produced the first machine calculations: transition from human computers to IBM machines (done in April/May '44).
  - Bethe led the *physics* part of the calculation: two methods (1) shock capturing (unsuccessfull), (2) shock tracking (successfull).
- CFD continued to be developed at Los Alamos (hydrogen bomb):
  - Compressible flow: Richtmyer (shock capturing), P. Lax (1949-50) and F. Harlow (1952).
- These three bodies of work formed the foundation for CFD, in particular for compressible aerodynamics, that Van Leer, Jameson and Roe among others built on.
- Later on, development of CFD spread outside Los Alamos, although significant achievements continued to took place there.

(Impressive) hand calculation in 1953

Kawaguti (1953) obtained the numerical solution for the flow around a circular cylinder at a *Reynolds* number of 40, using the full N-S equations, without a computer:

- Using the $\psi - \omega$ formulation and a non-uniform mesh with 232 nodes, he was able to achieve a remarkable accurate result.
- He wrote

  The numerical integration ... took about one year and a half with twenty working hours
  every week, with a considerable amount of labour and endurance.

C_D value	
Kawaguti (1953)	1.618
Present (ANSYS CFX)	1.614
Lima et al., J. Comp. Physics (2003)	1.54
Anderson, Exper. (1991)	1.8

(Impressive) hand calculation in 1953 - cont.

Left: Kavaguti (1953) - 232 nodes; right: ANSYS CFX - 33500 nodes.

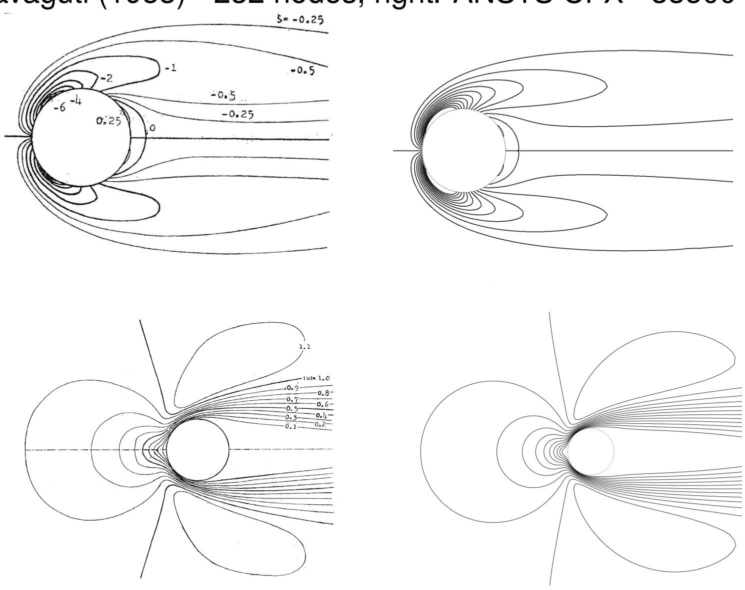

A brilliant CFD study ... *without* the computer!

Harlow and Fromm, Scientific American 1965

- *Scientific American* article of Harlow and Fromm (after *Physics of Fluids* 1965 article about *Marker and Cell* (MAC) method, later simplified in SMAC):
  - Striking, first-time visualizations of the 2D unsteady flow around a rectangular obstacle.
  - Enthusiastic - over-optimistic - view of the future of computer simulations.
  - Major impact in the scientific community.
  - Proved the capabilities of the new technology.

From left to right: mesh, streaklines and isotherms for the flow of air around a heated rectangular obstacle.

Fromm 1971

- Pioneering work of Fromm (*IBM J. Res. Develop.*, 1971) in the field of convective heat transfer.
  - Properly designed sophisticated finite difference system.
  - Performed the computation of the time-dependent, buoyant chaotic flow in a square cavity at values of the *Rayleigh* number as high as 10^{12}.
  - Several years before similar simulations were attempted by Paolucci, Le Quéré and Nobile.

From left to right: instantaneous streamlines, vorticity and isotherms for the buoyant flow in a square box at a *Ra* number of 10^8.

Programming languages

At the beginning, major part of code development was done *in-house*:

- Each research group had their own code(s), most of the times written in *FORTRAN IV*.
- Difficulties in implementing new models and algorithms.
- Programming done by experts in the specific thermal-fluid domain.
- Minor attention to readability, maintainability, proper documentation et.
- Corresponding codes were hard to read and interpret for those who did not write it - and even for those who wrote it after some time - with waste of time and resources.

Programming languages - cont.

Comparison of a piece of a FORTRAN code, modified by the present author in 1987, with a snippet of modern *Julia* code.

```
      PROGRAM COLL        73/172  OPT=0,ROUND= A/ S/ M/-D,-DS      FTN 5.1+6

          A(7*(MAXR/2)-6,5)=-XMAXR
          A(7*(MAXR/2)-6,8)=XMAXR**2/(XMAXR-1.0)
          A(3,6)=XMAXR
          A(7*(MAXR/2-1)-1,8)=-DIVZ
          A(7*(MAXR/2)-5,8)=-DIVZ
          A(7*(MAXR/2)-3,3)=HALFM
          A(7*(MAXR/2)-3,8)=-HALFM
          A(1,9)=HALFM*3.0
          A(1,13)=-HALFM*4.0
          A(1,16)=HALFM
          G1=CO1/GNUMBR
          G2=-G1*CO3
          CO8=CO3+1.0
          TCOMMN=G1*T(2,2)+CO2
          TALPHA=TCOMMN**(-CO3)
          TBETA=G2*TCOMMN**(-CO8)
          TONE=TBETA*(T(2,3)-T(2,2))
          TTWO=TBETA*(T(2,2)-T(1,2))*DIZSQ
          VONE=HALFM*V(2,2)
          TFOUR=TALPHA*3.0
          TSIX=TALPHA*DIZSQ
          A(2,13)=MONE*(TFOUR+0.5*TONE)-VONE
          UONE=DIVZ*U(2,2)
          A(2,9)=MONE*(TALPHA-0.5*TONE)+VONE+DIVRE*(TALPHA*MTWO+2.
         1-UONE
          A(1,12)=MONE*(TFOUR+TONE)-VONE
          VARIT=TALPHA*(DIZSQ-SQM2*6.0)
          A(1,8)=MONE*(TALPHA-TONE)+VONE+DIVRE*(VARIT+TTWO)-UONE
          SONE=V(2,2)*(-U(2,2)*DIVZ+DIVRE*(2.0*TSIX+TTWO))
          STWO=-DIVRE*(V(1,2)*TSIX+HALFM*DELTZ*TTWO*(U(2,3)-U(2,2
          B(1)=SONE+STWO
          UPORDN2=UP1+T(2,2)*(UP2+UP3*T(2,2))
          BONE=UPORDN2-DIVZ*(P(2,2)+U(2,2)**2)-U(1,2)*TALPHA*DIVR
          BTWO=DIVRE2*U(2,2)*(TSIX+TTWO)-DIVRE4*TONE*(V(2,2)-V(1,
          B(2)=BONE+BTWO
          TCOMMN=G1*T(2,MAXR)+CO2
          TALPHA=TCOMMN**(-CO3)
          TBETA=G2*TCOMMN**(-CO8)
          IF(ITALLY.EQ.0) GO TO 114
          TONE=TBETA*(T(2,MAXR)+HFLUXM-T(2,MAX1))
          GO TO 113
      114 TONE=0.0
      113 CONTINUE
```

```julia
using LinearAlgebra
using Random

function domeigen(A, p)
    b₀ = similar(A, size(A, 1))
    rand!(b₀)

    # power iteration
    bₖ = b₀
    for _ in 1:p
        bₖ₊₁ = A * bₖ

        # normalize
        bₖ = bₖ₊₁ / norm(bₖ₊₁)
    end

    # Rayleigh quotient
    λ = (A*bₖ ⋅ bₖ) / (bₖ ⋅ bₖ)

    return bₖ, λ
end
```

Real Programmers use FORTRAN!

Software development

Size of OpenFOAM and modeFRONTIER (2018R2):

Metric	modeFRONTIER	OpenFOAM
Lines of code	1.085.133	$\approx$ 1.000.000
Number of classes	12.668	-
Unit tests	23.586	-
Test coverage	36.1 %	-

Software Maintenance & Evolution:

➢ Big challenge for medium/small organizations.

➢ Highly expensive for bad quality software.

From structured to unstructured grids

- First general purposes codes based on single-block structured hexahedral grids:
  - (+) Efficient data structure and memory usage.
  - (-) Limited geometrical flexibility.
  - (-) Unsuitable to handling the complex geometries required for industrial applications.
- Finite Element Method (FEM), largely employed in structural analysis, had already the capability to handle arbitrary geometries through unstructured grids.
- Major effort towards development of unstructured grids for the Finite Volume Method (FVM).
- This culminated in the widely used cell-centered, collocated unstructured FVM with cells of arbitrary topology (Demirdžìc and Muzaferija, 1995).
- Approach adopted in most commercial and open source CFD packages, but it has disadvantages:
  - possible inaccuracies in the *reconstruction of the gradient*.
  - inefficient treatment of the diffusion term for complex, highly distorted grids.

An efficient cell-centered unstructured grid approach

B. Niceno (PSI) developed and tested a staggered, unstructured FVM for cells of arbitrary topology (ECCOMAS 2006):

- More demanding in terms of memory requirement and slightly more expensive, it has several favorable features:
  - No need of any stabilization procedure (Rhie & Chow, Arakawa, addition of 4^{th} Order dissipative terms et.) to couple velocity and pressure.
  - No need of *deferred correction*.
  - It is *(turbulence) energy conservative* (LES).

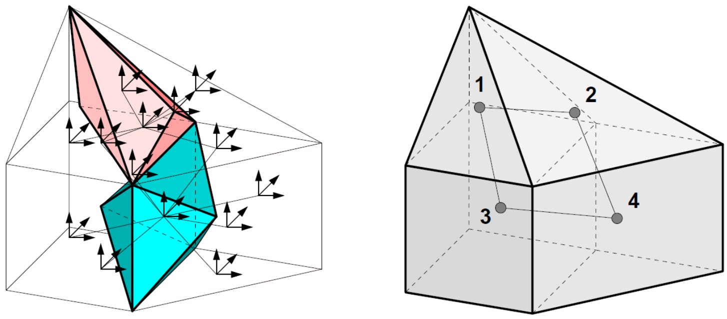

Finite Volumes for (left) momentum equation and (right) pressure equation.

Vector processors

- From the beginning of CFD, it was evident that its computational requirements was very high:
  - Intrinsic non-linearity of the governing equations.
  - Necessity to resolve boundary layers, regions with high gradients et.
- Mainframes available in the 1970s struggled to perform CFD calculations.
- Effort to develop faster computing platforms, which gave rise to the *vector processors*, e.g. CPUs that operate on 1D arrays of data.
- Cray family of vector supercomputers: Cray-1, Cray-XMP, Cray-YMP and Cray-2.
- Other companies: Control Data Corporation (Cyber 205), Fujitsu, Hitachi, Nippon Electric Corporation (NEC) et.,
- All, but NEC, abandoned the market and invested more on massively parallel machines.
- Experience in programming the IBM 3090 VF (Vector Facility) and Cray family (Cray-XMP and Cray-YMP):
  - Attainment of good performances with the IBM 3090 VF not an easy task.
  - Good performances on the Cray machines (time-dependent and chaotic flows).

Fortran coding on the CRAY X-MP, 1993

```
      subroutine add_correct(k_grid, vx, vy, prs, temp,
     .                        icvx, icvy, loff)
* I-----------------------------------------------------I
* I          C R A Y     V E R S I O N                  I
* I                                                     I
* I    1. UNROLLING OF A SHORT LOOP                     I
* I    2. FORCED VECTORISATION OF INNERMOST LOOP        I
* I-----------------------------------------------------I
*  Add corrections from the coarser to the actual grid....
*
      dimension vx(*), vy(*), prs(*), temp(*)
      dimension icvx(*), icvy(*), loff(*)
*
      do ikp1 = 2, icvy(k_grid+1)+1
CDIR$ IVDEP$
      do jkp1 = 2, icvx(k_grid+1)+1

         lockp1  = loff(k_grid+1)+(icvx(k_grid+1)+2)*
     +                 (ikp1-1)+jkp1
         ik      = 2*ikp1-2
         jk      = 2*jkp1-2
         lock1   = loff(k_grid)+(icvx(k_grid)+2)*
     +                  (ik-1)+jk
         lock2   = lock1+1
         lock3   = lock1+icvx(k_grid)+2
         lock4   = lock3+1
*
         vx(lock1)    = vx(lock1)   +  vx(lockp1)
         vx(lock2)    = vx(lock2)   +  vx(lockp1)
         vx(lock3)    = vx(lock3)   +  vx(lockp1)
         vx(lock4)    = vx(lock4)   +  vx(lockp1)
*        [.....]
      end do
      end do
*
      return
      end
```


Vectorized coupled solvers

- E. Nobile, Simulation of Time-dependent Flow in Cavities with the Additive Correction Multigrid Method, Part I: Mathematical Formulation, *Numerical Heat Transfer, Part B: Fundamentals*, **30**, No. 3, pp. 341-350, (1996).
- E. Nobile, Simulation of Time-dependent Flow in Cavities with the Additive Correction Multigrid Method, Part II: Applications, *Numerical Heat Transfer, Part B: Fundamentals*, **30**, No. 3, pp. 351-370, (1996).

(Loading video...) (Loading video...)

GPU

- Interest in vector processing revamped due to widespread availability of Graphic Processing Unit (GPU) and their increasing performances.
- GPUs include an array of shader pipelines which can be considered vector processors.
- Most HPC (High Performance Computing) manufacturers provide, among their offer, hybrid machines, e.g. CPUs+GPUs systems.
- Several CFD software vendors can - at least partially - exploit the GPUs if available.

Multiphase heat transfer

- Multiphase heat transfer: boiling, condensation, solidification et.
- Modeling of these phenomena is challenging!
- High-fidelity simulation - by e.g. DNS (Direct Numerical Simulation), LES (Large Eddy Simulation) or DES (Detached Eddy Simulation) - nowadays routinely performed for single-phase problems.
- *First principle* approach difficult, if not impossible, for many multiphase problems of scientific and practical interest.
- Reference book on direct numerical simulations of gas-liquid multiphase flows:

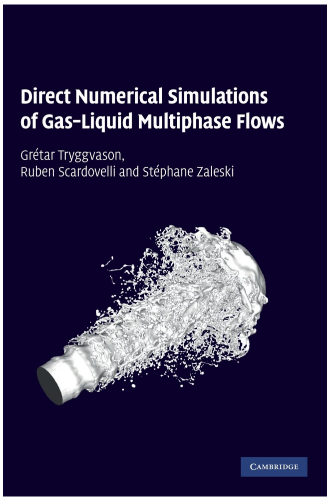

The beginning

- In 1969 B.D. Spalding, professor of Heat Transfer at Imperial College (IC), UK, founded the company *CHAM* (Combustion, Heat And Mass Transfer, Ltd., later superseded by Concentration, Heat And Mass Transfer, Ltd.).
- Gosman et al., *Heat and Mass Transfer in Recirculating Flows*, 1969.
- *PHOENICS* (Parabolic Hyperbolic Or Elliptic Numerical Integration Code Series) code from CHAM launched in 1978.
- *FLUENT* started in 1983 at Creare Inc. (Etna, NH, USA), by J. Swithinbank and F. Boysan at Sheffield University, UK:
  - Fluent Inc. founded in 1988, Lebanon, NH, USA.
  - In 1995, Fluent Inc. acquired by heat sink producer Aavid Thermal Technologies.
  - In 1996, Fluent Inc. acquired Fluid Dynamics International (FDI), Evanston, IL, which developed *FIDAP* (co-founded by M. Engelman and S. Rosenblat in 1982).
  - In 1997 acquired Polyflow S.A., a Belgian company developer of POLYFLOW.
  - Aavid acquired by Chicago private equity firm Willis Stein and Partners (WSP) in 1999 for US$ 260 million.

New players

- In the middle of 1980s, D. Gosman and R. Issa formed Computational Dynamics (CD) Ltd.:
  - Adapco backed CD to produce a body-fitted CFD code named *STAR-CD* (*Simulating Transport in Arbitrary Regions*).
  - First version block-structured but second release in 1991 unstructured (first unstructured commercial code).
  - *STAR-CCM+* launched after a development phase commenced in 1999.
  - *CD-Adapco* acquired by Siemens in 2016 for $970 million.
- UK's Atomic Energy Authority (AEA) privatized a portion of itself in 1996 as *AEA* Technology, which contained their CFD business, *Harwell-FLOW3D*, later renamed to *CFX*:
  - Up to Rel. 2 of Harwell-FLOW3D limited to curvilinear, single-block structured grids.
  - In 1993, with Rel. 3.2, it added multi-block capability.
  - Development of their unstructured code (*ASTEC*) abandoned after acquisition of *TASCflow* from Advanced Scientific Computing (ASC) of Waterloo, Ontario, CDN.
- ANSYS, renowned for its structural analysis tools:
  - In 2003 acquired the of CFX division of AEA technology (ICEM CFD was acquired in 2000).
  - Purchased *Fluent* from WSP in 2006 for US$ 630 million.
  - Had to obtain FTC (Federal Trade Commission) clearance for the Fluent acquisition.

Other players, M&A

A *not-exhaustive* list:

- Flow Science Inc. (FLOW-3D)
- Numeca (Fine, Omnis)
- ESI (ACE+, ESI-PRESTO, Systus, Visual-CFD for OpenFOAM)
- Convergent Science (CONVERGE CFD)
- Siemens (STAR-CCM+)
- Autodesk (Autodesk ® CFD)
- Dassault Systèmes (Abaqus/CFD, XFlow, SCStream, PowerFLOW® CFD
- SOLIDWORKS® Flow Simulation, Simerics MP for SOLIDWORKS)
- MSC (scFLOW, scSTREAM, sc/Tetra)
- AVL (AVL FIRE™).

Web browser based simulation (es. SimScale).

Harwell-FLOW3D-Rel. 2

- Purchased (tapes...) in 1990.
- Deployed at the University of Trieste Central Computing Center (Centro di Calcolo):
  - Grid generator, Pre- and Post-processor on a Digital VAX VMS 780.
  - Solver on a CRAY X-MP/14se: theoretical peak performance of 200 Mflops.
  - Iphone 7 Plus (12 Pro Max), Multithreaded mode enabled/disabled, LINPACK 1000×1000: *6570/3450* (*10589/5035* Mflops.

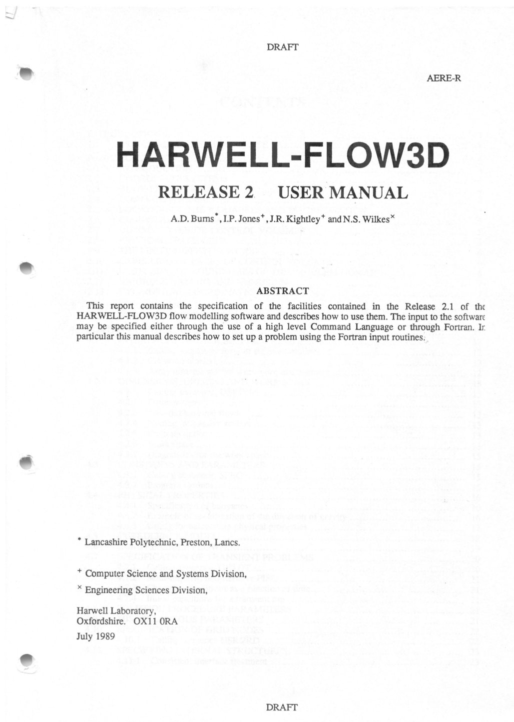

DRAFT

AERE-R

HARWELL-FLOW3D

RELEASE 2 USER MANUAL

A.D. Burns*, I.P. Jones+, J.R. Kightley+ and N.S. Wilkes×

ABSTRACT

This report contains the specification of the facilities contained in the Release 2.1 of the HARWELL-FLOW3D flow modelling software and describes how to use them. The input to the software may be specified either through the use of a high level Command Language or through Fortran. In particular this manual describes how to set up a problem using the Fortran input routines.

* Lancashire Polytechnic, Preston, Lancs.

\+ Computer Science and Systems Division,

× Engineering Sciences Division,

Harwell Laboratory,
Oxfordshire. OX11 0RA
July 1989

DRAFT

Iridotomy, 1991

- Evaluation of the effect of iridotomy's diameter in the reduction of pressure difference between anterior and posterior chambers of the eye for patients suffering from acute glaucoma.
- Among one of the first CFD applications in this particular field.

- Computational domain, axial-symmetric grid and detail of the velocity field for an iridotomy diameter of 100 μm:

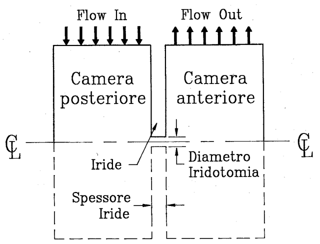

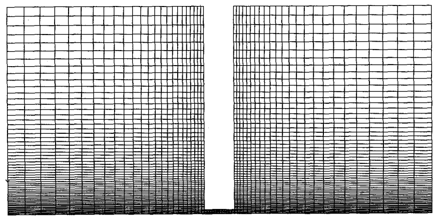

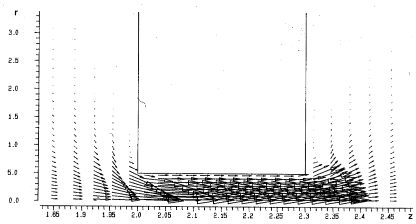

CFD Open Source

Usually provided under a software license that permits users to study, change, and improve the software.

- Most widely used open-source CFD software package is *OpenFOAM*:
  - Official *OpenFOAM* release maintained by the *OpenFOAM Foundation*.
  - Some companies have developed code variations to commercialize their additions to the code.
- *SU2*, developed mainly at Stanford University and particularly oriented towards external aerodynamics.
- *Basilisk*, successor of the *Gerris* flow solver:
  - Strong capabilities in modelling multiphase, free surface flows.
  - Use of quad-tree (in 2D) and oct-tree (in 3D) adaptive grids.
- *Palabos* CFD solver:
  - Based on the Lattice-Boltzmann Method (LBM).
  - New product OMNIS™/LB from Numeca integrated *Palabos* in a monolithic enhanced configuration, with a large range of functionalities.

NASA CFD Vision 2030

NASA/CR-2014-218178 - CFD Vision 2030 Study: A Path to Revolutionary Computational Aerosciences

- Provides a *knowledge-based forecast of the future computational capabilities required for turbulent, transitional, and reacting flow simulations...*.
- Not strictly related to CHT, but might be of interest to the thermo-fluid community.
- Some of the topics of the NASA document are addressed in the following, together with others which might be of specific interest to CHT.

Multiobjective and robust optimization

- Use of *optimization* methods has gained more acceptance within the Heat Transfer community, with applications ranging from component to system level.
- Presence of uncertain model data, e.g. initial and boundary conditions, thermo-physical properties of the medium and uncertainties (tolerances) in geometrical dimensions:
  - Need for efficient uncertainty quantification (UQ) for establishment of confidence intervals in computed predictions.
  - Optimization under uncertainty, e.g. *robust* optimization.

Shape optimization of a tube bundle in cross-flow

- Ranut et al., *Multi-objective shape optimization of a tube bundle in cross-flow*, 2014:
  - Three simultaneous - and conflicting - objectives considered, e.g. Maximization of the heat transfer rate outside the tubes, minimization of the pressure loss for the external flow and minimization of the pressure loss for the internal flow.
  - Sketch of the problem, tube shape parametrization and domain used for the periodic simulation at the shell side:

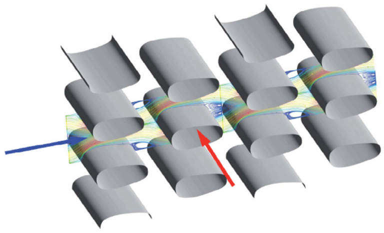

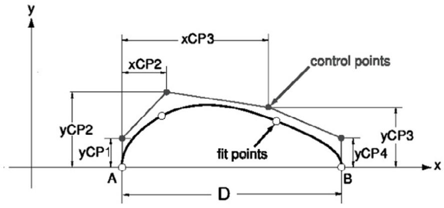

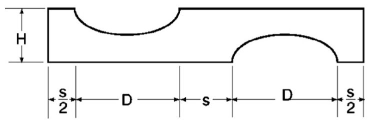

Shape optimization of a tube bundle in cross-flow - cont.

2D visualizations of the objective space Δp_{tube} - ΔP_{shell} and ΔT_{per} - Δp_{shell} together with some of the optimal designs and visualizations of flow and temperature fields for design number 894.

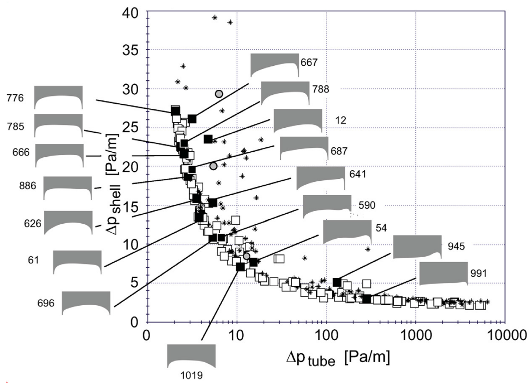

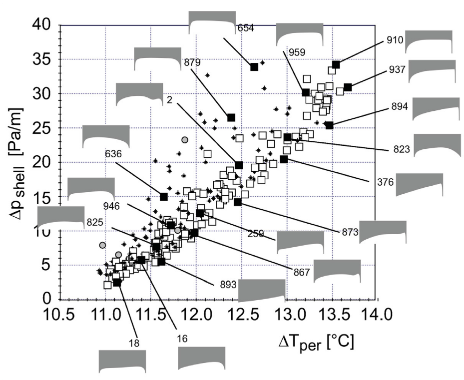

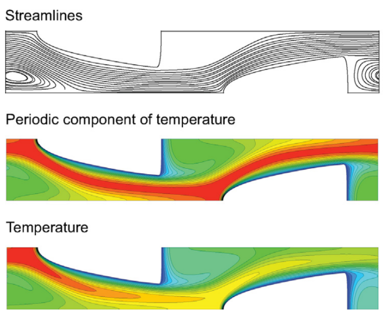

Low vs High order methods

- Many industrial - commercial or open source - CFD and CHT tools based on cell-centered or node-(vertex) centered FVM:
  - Limited in most cases to 2^{nd} order discretization of the underlying conservation equation.
  - Practical applications frequently require tens or even hundreds of million mesh points.
- Increasing interest in *Scale resolving simulations*, like *LES* (Large Eddy Simulations) and *DES* (Detached Eddy Simulations), for practical problems:
  - Can require very fine meshes and thousands of small time steps to resolve the energy containing part of the turbulence spectrum and to achieve significant statistical results.
- Use of *high order* methods - order greater or equal to three - would be extremely beneficial, since the reduction in the number of grid points would more than compensate the increase of the computational cost.
- High-order methods are in general less robust and more prone to instabilities and convergence difficulties.
- Major effort in the development of high-order CFD methods, e.g. EU funded project *IDIHOM* (Industrialisation of high-order methods).
- Review of high order methods by Huynh et al., 2014:
  - Proposed Flux Reconstruction (FR) approach or Correction Procedure using Reconstruction (CPR).
  - Unifies the most important high-order methods, i.e. Discontinuous Galerkin (DG), Spectral Difference (SD) and Spectral Volume (SV) methods.

Multiscale simulations

- Several heat transfer and fluid flow problems are *multiscale*:
  - Thermal control in a data center.
  - Fuel cells.
- *Multiscale numerical methods* are needed.
- Include macroscopic standard continuum methods, e.g. Navier-Stokes and energy equations; mesoscopic particle-based lattice Boltzmann, direct simulation Monte Carlo, dissipative particle dynamics and microscopic molecular dynamics.
- Recent (2019) review of Tong et al. provides an extensive review of current progresses of the multiscale simulations for fluid flow and heat transfer problems.

Do we need a mesh ?

- In traditional methods, like i.e. FVM and FEM, nodes (or cell centroids) are connected to a certain number of neighbors through a *mesh* or *grid*:
  - For cell-centered FVM, the grid defines the geometric properties of each cell and the *connectivity* between the centroids.
  - Connectivity required to construct mathematical operators, e.g. the *gradient*.
- The mesh must possess certain requisites, i.e. degree of orthogonality, minimum skewness et., to guarantee accurate and stable simulations.
- In some situations these requisites are hard to maintain and lead to either increase of computational costs or catastrophic failures.

Why meshless

- *Meshless* or *Meshfree* methods: avoid any mesh at all, and compute directly the interaction of each node with some of its neighbors which are typically within a given distance.
- *Meshless* methods enable the computation of some otherwise difficult problems, at the cost of some extra computing time and programming effort (till now).
- Absence of a mesh allows *Lagrangian simulations*, in which the nodes can move according to the velocity field.

Meshless methods

Several *meshless* methods for CFD and CHT applications:

- ➢ *SPH* - Smooth particle hydrodynamics.
- ➢ *MPS* - Moving particle semi-implicit.
- ➢ *PIC* - Particle-in-cell.
- ➢ *MLS* - Moving least squares.
- ➢ *LRBFCM* - Local radial basis function collocation method, also known as radial basis function generated finite differences (*RBF-FD*) method.

Example of use of *MPS*

Use of *MPS* (Particleworks) methos for the simulation of cooling of a medium speed engine piston (courtesy of S. Ojala):

- Instantaneous position of fluid particles and computed time-averaged heat transfer coefficient.
- Fluid particles represent the oil jet used to cool the piston.
- Free surface and surface tension.

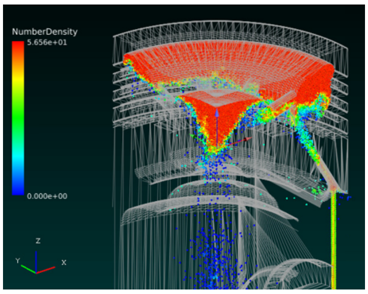

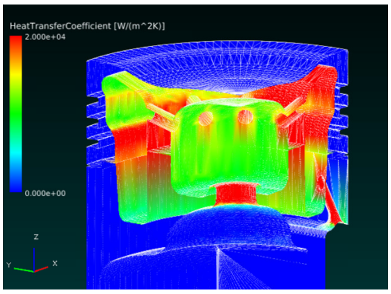

Simulation time comparison:

Parameter	MPS (Particleworks)	VOF
Physical time (one piston stroke) [s]	0.1	0.1
Part. diam. (MPS)/avg. cell size (VOF) [mm]	1.75	2
N. CPU/GPU cores	2 CPUs / 1 GPU	160 CPUs
Simulation time [h]	5	24

LRBFCM @UniTS

- Development of LRBFCM at University of Trieste (R. Zamolo, B. Šarler):
  - Techniques to place the nodes in a very general and flexible way.
  - Increase the computational performances of the method.
- Images approximated through the *stippling* technique:

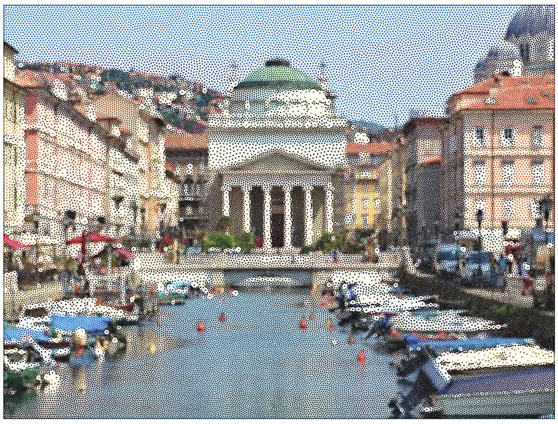

LRBFCM @UniTS - *cont.*

UIT Heat Transfer Conference 2019

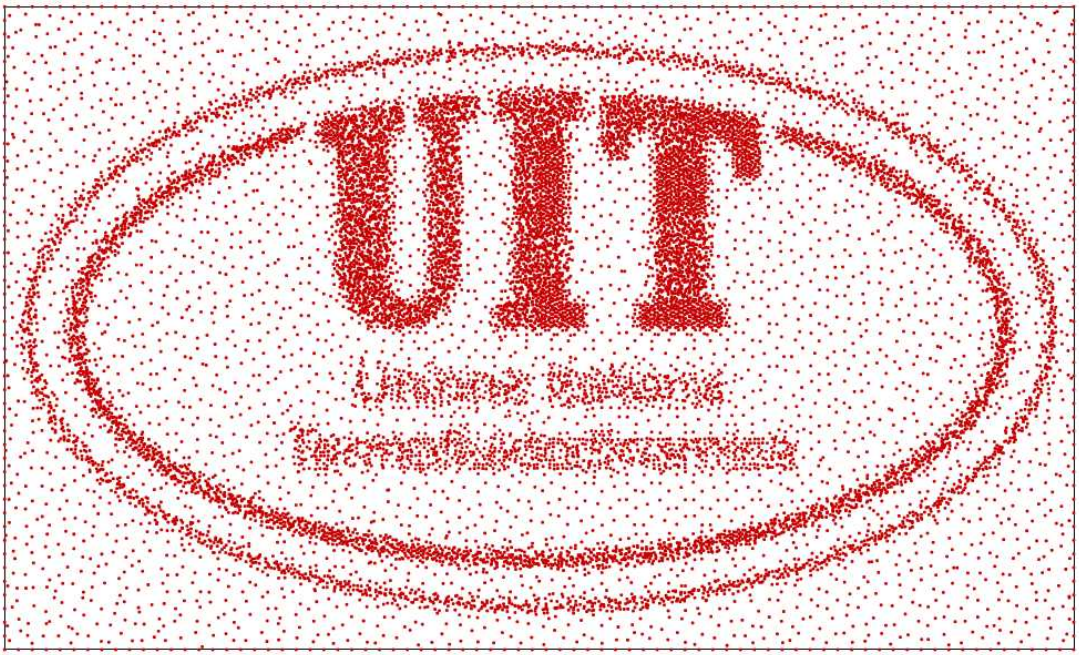

LRBFCM @UniTS: examples

Backward facing step

- Computational domain

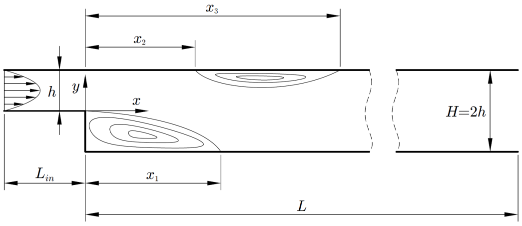

- Details of nodes distribution

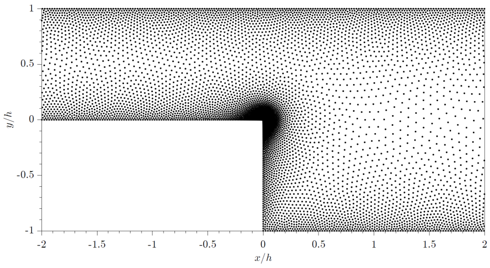

Microchannel

- Computational domain

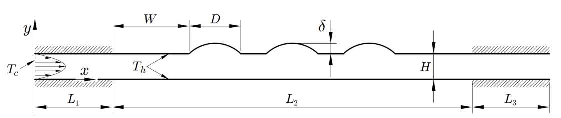

- Details of nodes distribution

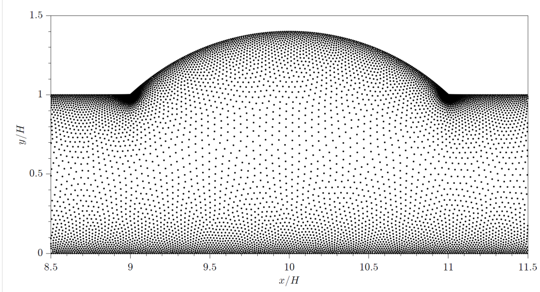

LRBFCM @UniTS: examples- *cont.*

Flow around a cylinder at $Re = 2000$ and buoyant flow in a square cavity at $Ra = 4 \times 10^8$:

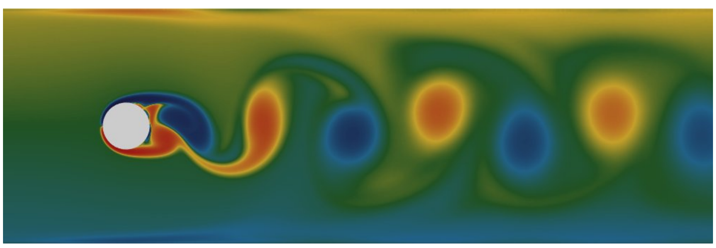

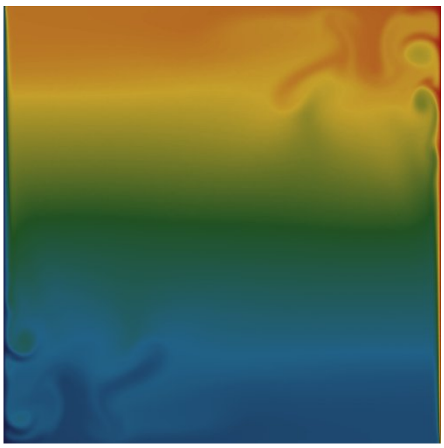

Machine Learning and AI

- *Machine learning* (ML): algorithms and statistical models that computers use in order to perform a specific task without using *explicit instructions*, but rather relying on *patterns*.
- ML algorithms build a mathematical model based on sample data (*training data*) in order to make predictions without being explicitly coded to perform the task.
- ML and *optimization*: minimization of some loss function on a training set of examples.
- Growing interest of ML models in thermal fluid simulation:
  - Advent of data-intensive thermo-fluid experiments and high-fidelity numerical simulations.
  - Affordable computing platforms.
  - Progress in ML methods: deep learning using multilayer neural networks (NN).
- With reference to CFD and CHT, ML can be defined as the capability to create effective *surrogates* from a massive amount of data (measurements and/or simulations).
- Concept of *physics-informed neural networks*.

ML example: boiling

Liu et al. (ATE, 2018) used a deep feedforward neural network (DFNN) to predict boiling heat transfer:

- Inputs: local momentum and energy convective transport, pressure gradients, turbulent viscosity, surface information.
- Outputs: quantities of interest (heat transfer components, wall superheat, near wall void fraction).
- Networks trained by high-fidelity data from first principle simulation of pool boiling.

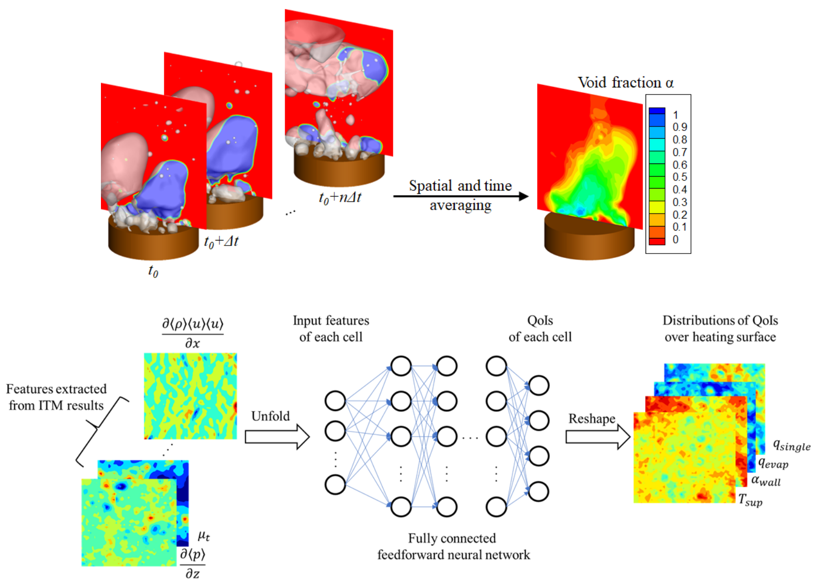

ML example: boiling - cont.

Predictive capability of the DFNN by comparison between DFNN predictions and the original ITM (Interface Tracking Method) results on the heating surface:

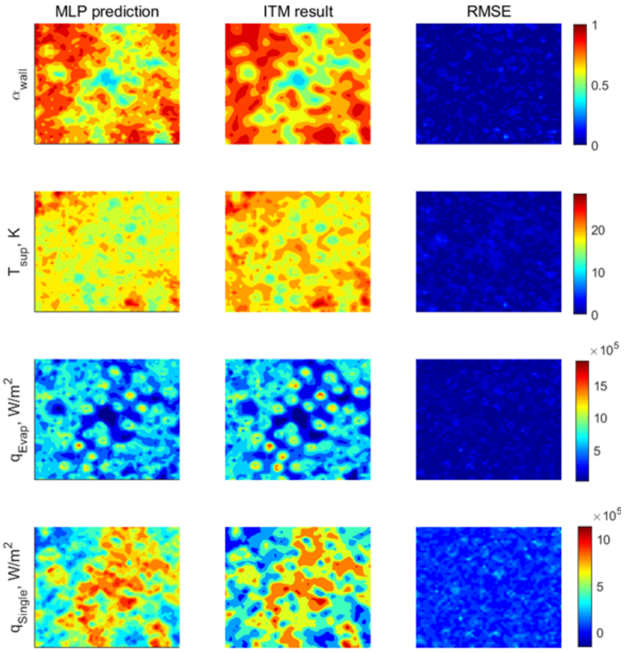

The DFNN prediction captures both the local boiling process and the global boiling pattern
with good accuracy.

What's next ?

- Some milestones in the history of CFD (review *biased* by personal experience).
- From an esoteric discipline to an advanced technology for the aeronautical and nuclear sector, CFD and CHT eventually went mainstream, with pervasive applications in almost any field.
- Different level of maturity of CFD and CHT.
- Fundamental and applied research required to advance the credibility level in e.g. turbulence, multiphase flows, et.
- While noteworthy progress has been obtained, in some cases the experimental methods still represent the most reliable tools.
- Dramatic increase of performance of computing hardware in recent years.
- Lag of software: legacy codes, which in some cases date back to the 80's, are still the workhorse in several research applications.
- New and exciting opportunities for research:
  - ➢ Relentless increase of performance of novel dedicated hardware.
  - ➢ Development of new numerical algorithms.
  - ➢ New programming paradigms.
  - ➢ Machine learning and AI technologies.
  - ➢ Quantum computing.

What's next ? Is *Quantum Computing* the next revolution for CFD??

It seems that, from many sources, *Quantum Computing* (QC) is the key-enabler for (almost) real-time, ultra-high resolution (DNS) for CFD. Is this true?

- ... *It is clear that the era of QC is here ... the CFD community, along with other aeroscience and engineering communities, needs to recognize this evolution and understand that this is not a short-term endeavor.* [*AIAA JOURNAL* Vol. 58, No. 8, August 2020 - Quantum Speedup for Aeroscience and Engineering, P. Givi, A.J. Daley, D. Mavriplis, M. Malik].
- ... *Finally, let us consider the IBMQ 54-qubit machine for some specific remarks.* ... *2. DNS grid sizes: With a 54-qubit machine we can store and compute on*
  1. 1D: $\leq 10^{16}$ meshes
  2. 2D: $\leq 10^{8} \times 10^{8}$ meshes
  3. 3D: $\leq 10^{5} \times 10^{5} \times 10^{5}$ meshes

  Here, each of these mesh sizes is far higher than the largest available DNS computations at present. [*Indian Academy of Sciences Conference Series* (2020) 3:1 - Quantum computation of fluid dynamics, S.S. Bharadwaj, and K.R. Sreenivasan].

But...

- ... *In actual practice, QC ensemble simulations of the Navier?Stokes equations demand hundreds of noiseless logical qubits. Given that current quantum computing typically works only up to a few logical qubits, say of the order ten, the target appears pretty much into the future.* [*Computers and Fluids* 270 (2024) 106148 - S. Succi, W- Itani, C. Sanavio, K.R. Sreenivasan, R. Steijl]

OUTLINE

Parte III

Applications

10 Esempi
- Eliche navali
- Turbina Pelton
- Stirrer elettromagnetici
- Numerical Analysis of Convection in Metal Foams
- Simulazione di incendio e propagazione fumi
- L'uso della modellazione CFD nella medicina Cardiovascolare

Cavitazione

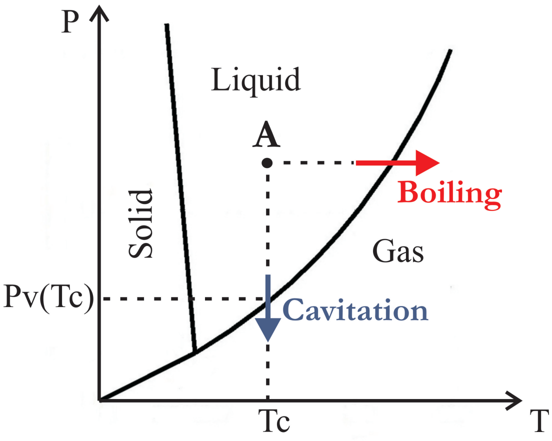

La *cavitazione* può essere definita come:

- La vaporizzazione di un liquido quando la pressione (statica) scende a valori inferiori a quelli della corrispondente pressione di saturazione [1]
- La formazione ed attività di bolle - o cavità - in un liquido [2]
- Il *collasso* (breakdown) di un liquido in condizioni di pressione molto bassa [3]

[1] Coutier-Delgosha, O., Reboud, J., Delannoy, Y., Numerical simulation of unsteady behaviour of cavitating flows, *Int. J. Num. Meth. Fluids*, **42**, pp. 527-548, (2003).

[2] Young, F., *Cavitation*, Imperial College Press, London, (1989).

[3] Franc, J., Michel, J., *Fundamentals of Cavitation*, Kluwer Academic Publisher, (2004).

Esempi di cavitazione idrodinamica

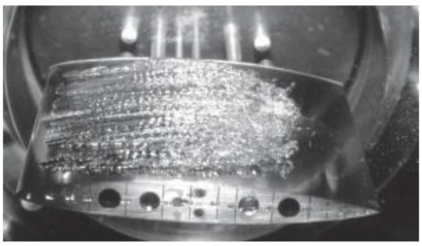

Partial Cavitation
(Cavitazione parziale)

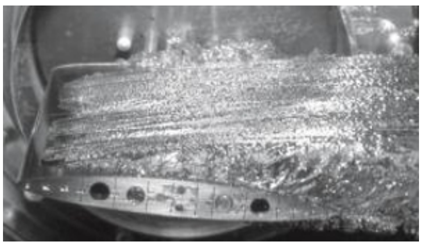

Supercavitation
(Supercavitazione)

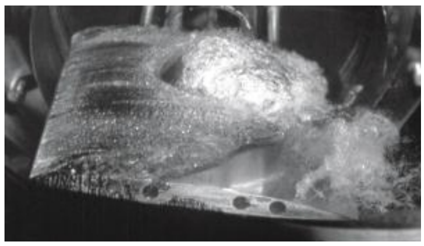

Cloud Cavitation
(Cavitazione a nuvola)

Bubble Cavitation
(Cavitazione a bolle)

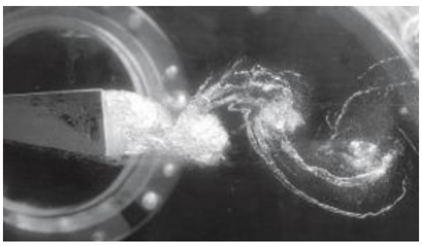

Vortex Cavitation
(Cavitazione a vortice)

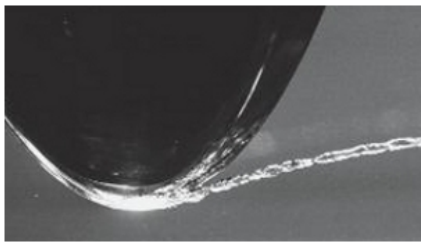

(Tip) Vortex Cavitation (Cavitazione sul vortice del bordo d'attacco)

Figure tratte da: *Fluid Dynamics of Cavitation and Cavitating Turbopumps*. Edited by D'Agostino, L., and Salvetti, M.V., 2007

Elica E779A

- Test case per la *validazione* di codici/procedure CFD;
- Proprietà di CNR-INSEAN (The Italian Ship Model Basin) `http://www.insean.it/`;
- Diametro D = 0.2272 m

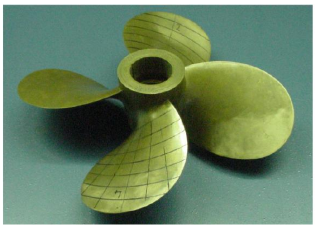

Elica E779A

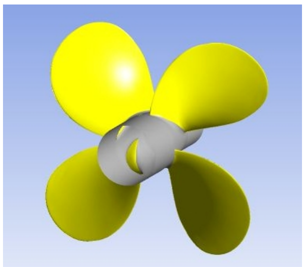

Elica E779A: modello CAD

- Simulazioni stazionarie;
- Approccio MRF (Multiple Reference Frame);
- Dominio diviso in due parti:
  - Parte rotante: *Rotating*
  - Parte stazionariat: *Fixed*

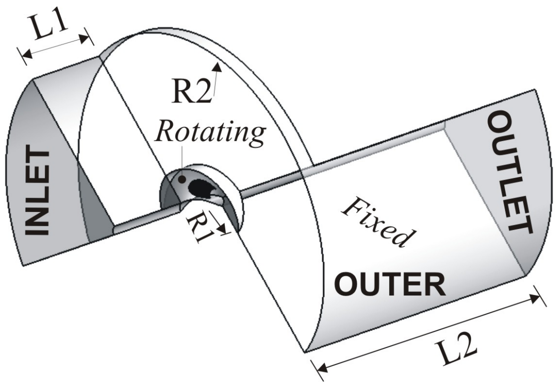

Dominio di calcolo

Propeller E779A - Cavitation Patterns

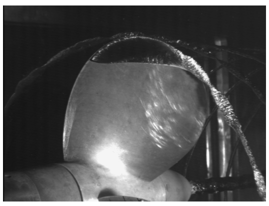

Exp. J=0.71, $\sigma_n = 1.763$

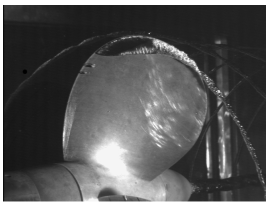

Exp. J=0.77, $\sigma_n = 1.783$

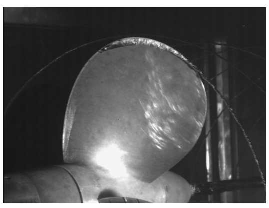

Exp. J=0.83, $\sigma_n = 2.063$

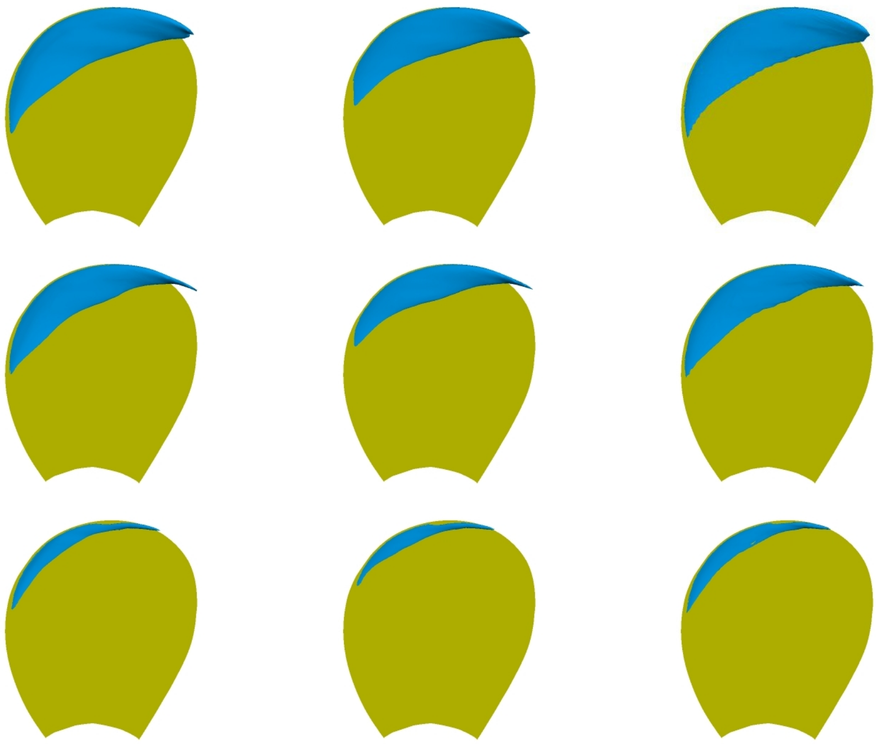

Zwart FCM Kunz

$$J = \frac{V}{nD} \qquad \sigma_n = \frac{P_{ref} - P_v}{0.5\rho_l (nD)^2}$$

Elica E779A - Spinta e momento torcente

Numerical results at J=0.71 for $\sigma_n = 1.763$
and for the non cavitating regime

	Non-Cavitating		Cavitating	
	Kt	Kq	Kt	Kq
Measured	0.256	0.464	0.255	0.46
SST	0.246	0.442		
Zwart+SST			0.252	0.453
FCM+SST			0.249	0.446
Kunz+SST			0.253	0.453
RSM	0.247	0.441		
Zwart+RSM			0.252	0.450
FCM+RSM			0.249	0.443
Kunz+RSM			0.253	0.451

$$J = \frac{V}{nD} \qquad \sigma_n = \frac{P_{ref} - P_v}{0.5\rho_l (nD)^2}$$

$$Kt = \frac{T}{\rho_l n^2 D^4} \qquad Kq = \frac{Q}{\rho_l n^2 D^5}$$

SST = Shear Stress Transport

RSM = Baseline Reynolds Stress Model

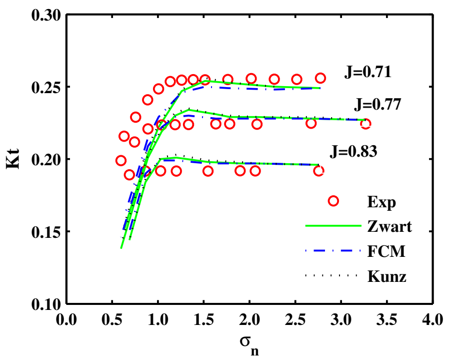

Influence of the cavitation number σ_n and of the mass transfer model on the thrust coefficient.

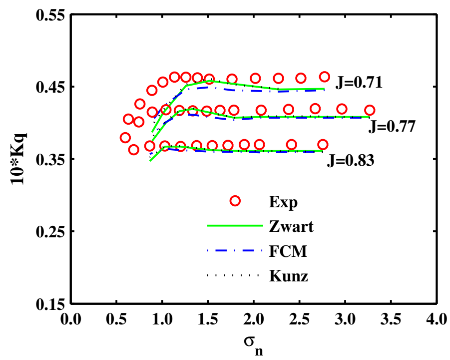

Influence of the cavitation number σ_n and of the mass transfer model on the torque coefficient

SMP11 - Workshop Propeller performance

Second International Symposium on Marine Propulsors 2011
Workshop: Propeller performance
17 - 18 June 2011, Hamburg, Germany

- Potsdam Propeller Test Case (PPTC)
- Cavitation Tests with the Model Propeller VP1304
- Case 2.3
- Blind Benchmark
- Proceedings available on-line:
`http://www.marinepropulsors.com/smp/files/downloads/smp11_workshop/smp11_workshop/`

SMP11 - Workshop Propeller performance

Eleven participating groups

Group	Solver	Acronym
Berg-Propulsion	Procal	Berg-Procal
Cradle	SC/Tetra	Cradle-SC/Tetra
CSSRC	ANSYS Fluent	CSSRC-Fluent
HSVA	QCM	HSVA-QCM
	PPB	HSVA-PPB
INSEAN	PFC	INSEAN-PFC
SSPA	ANSYS Fluent	SSPA-Fluent
TUHH	FreSCO+	TUHH-FreSCO
University of Genua	Panel	UniGenua-Panel
	StarCCM+	UniGenua-StarCCM
University of Triest	ANSYS CFX(FCM)	UniTriest-CFX(FCM)
	ANSYS CFX(Kunz)	UniTriest-CFX(Kunz)
	ANSYS CFX(Zwart)	UniTriest-CFX(Zwart)
VOITH	Comet	VOITH-Comet
VTT	FinFlo	VTT-FinFlo

SMP11 - Propeller PPTC

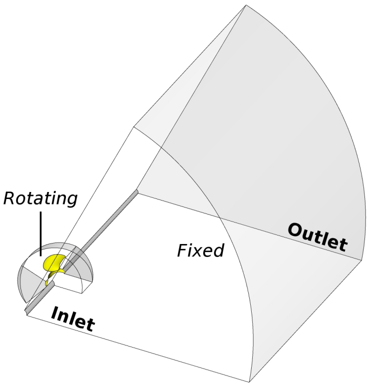

Computational Domain

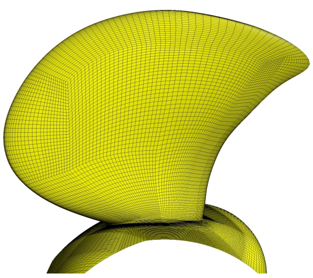

Blade surface mesh

- Steady state simulations
- MRF approach
- SST turbulence model
- Domain split in two parts
  - Rotating Part: *Rotating*
  - Stationary Part: *Fixed*
- *Rotating* = 1838655 nodes
- *Fixed* = 275680 nodes

SMP11 - Cavitation patterns

Experiment

UniTriest-CFX(FCM)

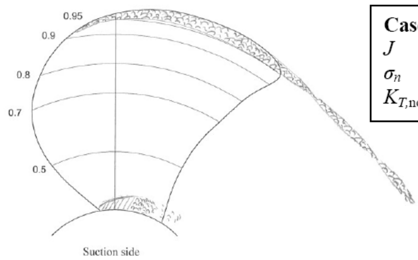

Case 2.3.1	
J	$= 1.019$
σ_n	$= 2.024$
$K_{T,\text{no cav.}}$	$= 0.387$

Calculation

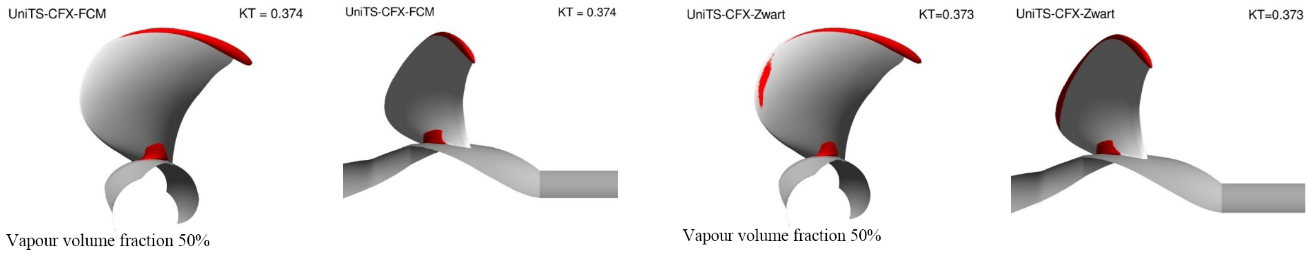

SMP11 - Cavitation patterns

Experiment

UniTriest-CFX(FCM)

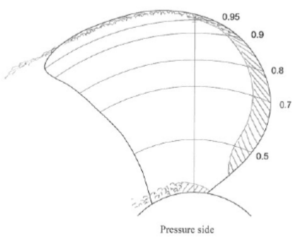

Case 2.3.3	
J	$= 1.408$
σ_n	$= 2.000$
$K_{T,\text{no cav.}}$	$= 0.167$

Calculation

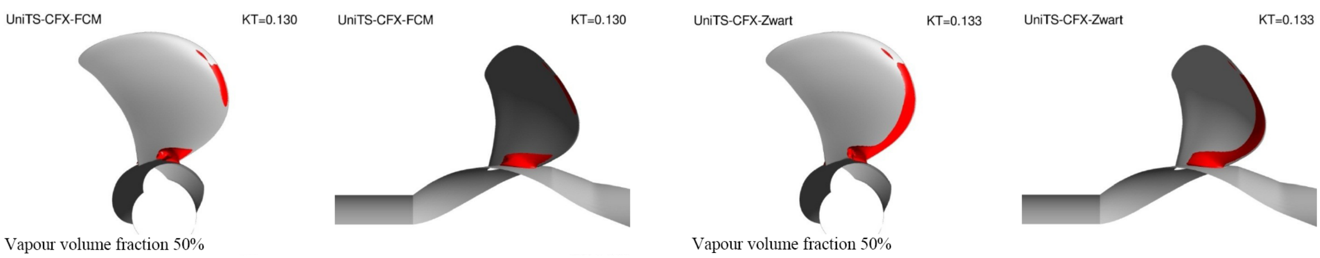

SMP11 - Thrust coefficient

Table 3: Thrust coefficients of cavitating propeller

	case 2.3.1 K_T [-]	case 2.3.2 K_T [-]	case 2.3.3 K_T [-]
Exp. (non-cavitating)	**0.3870**	**0.2450**	**0.1670**
Exp. (cavitating)	**0.3725**	**0.2064**	**0.1362**
Berg-Procal	0.3760		
Cradle-SC/Tetra	0.3750	0.1990	0.1380
CSSRC-Fluent	0.3740	0.1940	0.1320
INSEAN-PFC	0.3570	0.2330	0.1610
SSPA-Fluent	0.3880	0.2050	0.1440
TUHH-FreSCO+	0.3830		0.1440
TUHH-FreSCO+ (small-large coef.)		0.2420 - 0.1370	
UniGenua-Panel	0.3922	0.2369	0.1378
UniGenua-StarCCM	0.3782	0.2035	0.1306
UniTriest-CFX(FCM)	0.3740	0.2030	0.1300
UniTriest-CFX(Kunz)	0.3750	0.2100	0.1330
UniTriest-CFX(Zwart)	0.3730	0.1960	0.1330
VOITH-Comet	0.3852	0.2101	0.1513
VTT-FinFlo	0.3860	0.2020	0.1420

SMP11 - Thrust differences

Table 4: Difference between computed and measured thrust of cavitating propeller

	case 2.3.1 ΔK_T [%]	case 2.3.2 ΔK_T [%]	case 2.3.3 ΔK_T [%]
Berg-Procal	0.94		
Cradle-SC/Tetra	0.67	-3.59	1.32
CSSRC-Fluent	0.40	-6.01	-3.08
INSEAN-PFC	-4.16	12.89	18.21
SSPA-Fluent	4.16	-0.68	5.73
TUHH-FreSCO+	2.82		5.73
TUHH-FreSCO+ (small-large coef.)		17.25 - -33.62	
UniGenua-Panel	5.29	14.78	1.17
UniGenua-StarCCM	1.53	-1.41	-4.11
UniTriest-CFX(FCM)	0.40	-1.65	-4.55
UniTriest-CFX(Kunz)	0.67	1.74	-2.35
UniTriest-CFX(Zwart)	0.13	-5.04	-2.35
VOITH-Comet	3.41	1.79	11.09
VTT-FinFlo	3.62	-2.13	4.26

E779A propeller, non-homogeneous inflow

Experimental setup

E779A, tunnel set-up. Picture taken from [1].

- Operational condition, J = 0.90, (σ_n = 4.455)
  Propeller diameter, D = 0.227 m
  Free-stream inlet velocity, V = 6.22 m/s
  Propeller rotation speed, n = 30.5 rps
  Water density, ρ_L = 998 kg/m^3
  K_T (mean) = 0.175

[1] Salvatore, F, The INSEAN E779A propeller Experimental Dataset.EU-FP6., Project VIRTUE, Deliverable D4.1.3

E779A propeller, non-homogeneous inflow

Numerical setup

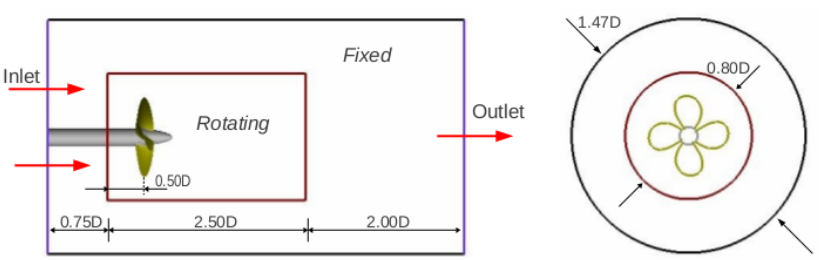

Geometry of the computational domain

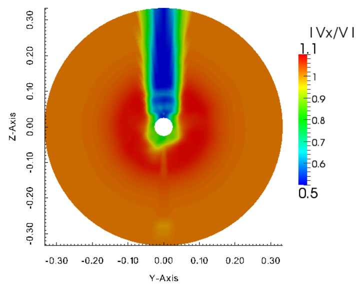

Nominal wake on the Inlet boundary.

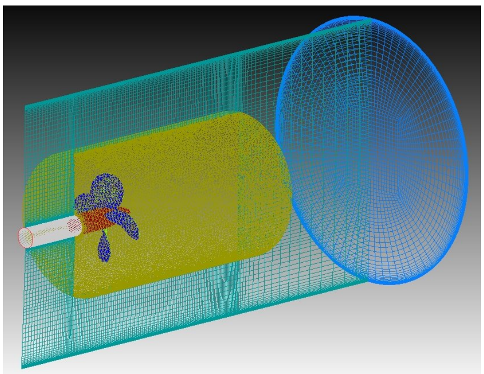

Computational grid

Characteristics of the computational grid

Computational grid		
Rotating		
	number of prisms:	708,000
	number of tetrahedra:	2,012,222
	total number of cells:	2,720,222
Fixed		
	total number of hexahedral cells:	394,839
Total number of cells:		3,115,061

E779A propeller, non-homogeneous inflow

Countours of the axial velocity

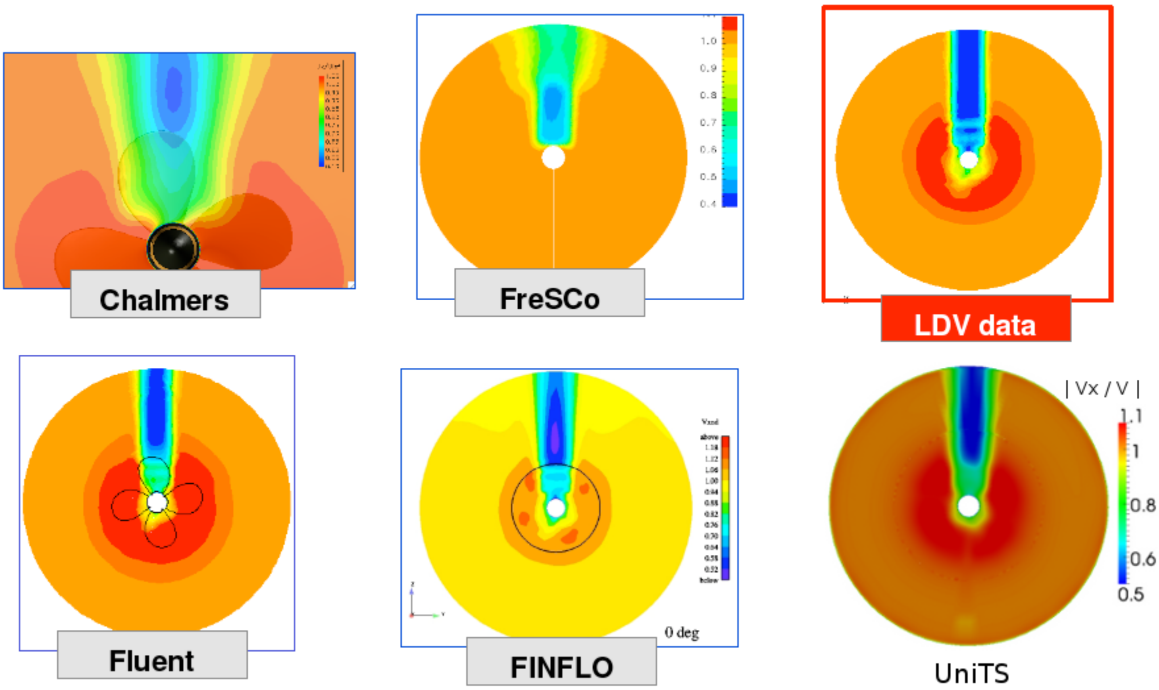

Axial velocity measured/computed in a plane 0.26D upstream of the propeller mid plane. Picture adapted from [2].

International Symposium on Cavitation, smp'09, Trondheim, Norway, pag. 362-371

E779A propeller, non-homogeneous inflow

Contours of Cp=-3.0

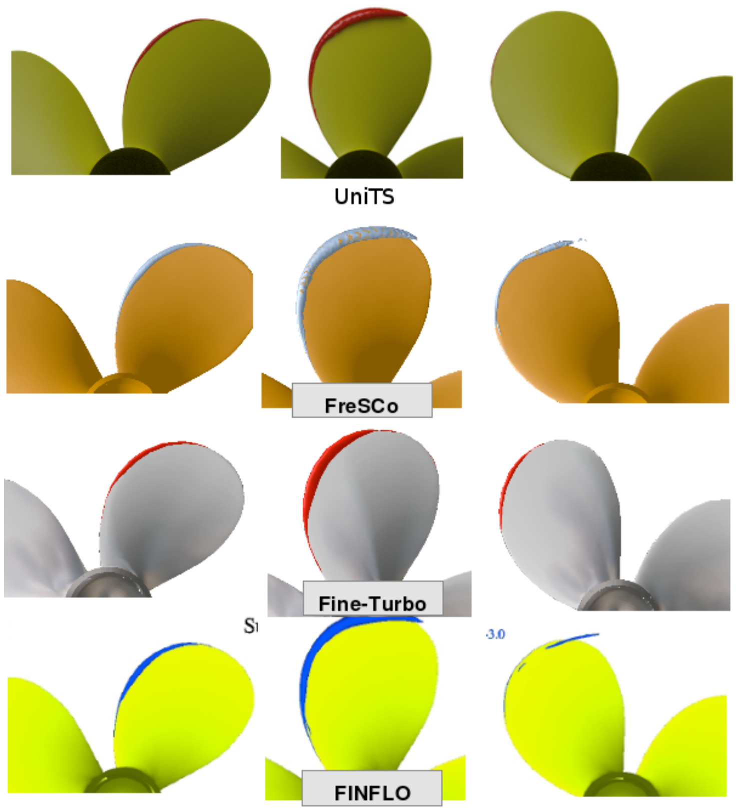

E779A propeller, non-homogeneous inflow

Cavity evolution

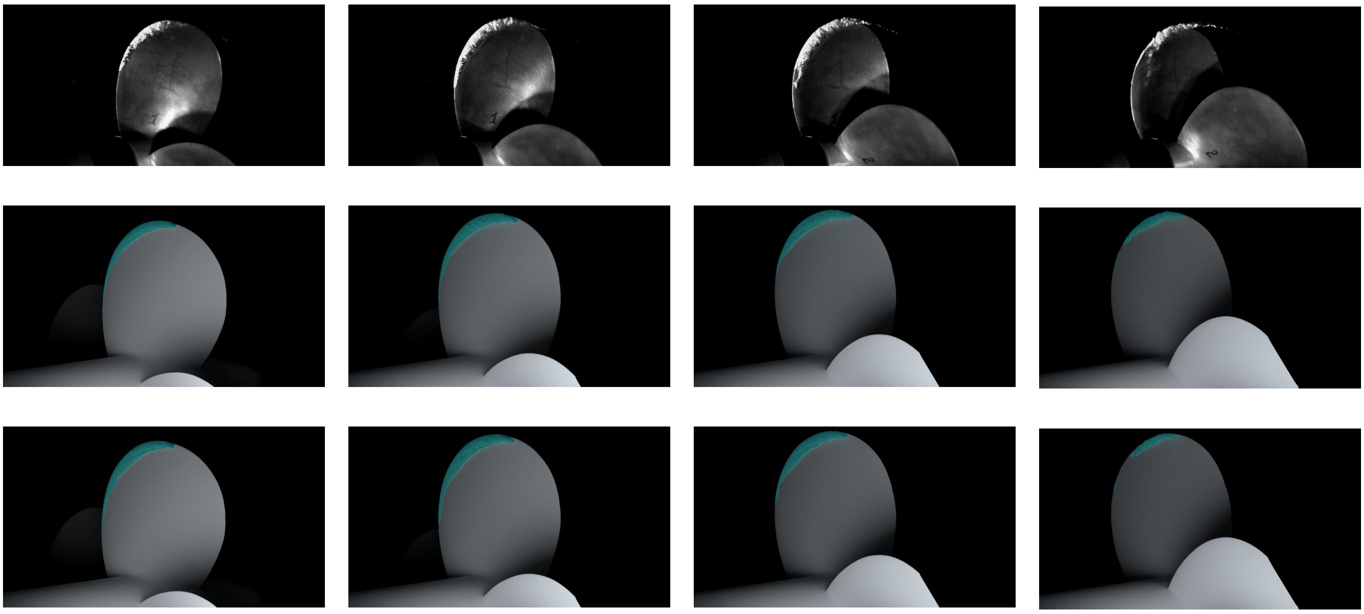

-10° | 0° | 10° | 20°

Cavity evolution with propeller rotation. Experimental data (top). Results obtained with calibrated FCM (middle) and with calibrated Kunz model (bottom).

E779A propeller, non-homogeneous inflow

(Loading video...)

Turbina Pelton - 1

Per gentile concessione Dott.ssa Dragica Jošt, *Turboinštitut, Ljubljana, SLO*

Modello sperimentale:

Modello numerico:

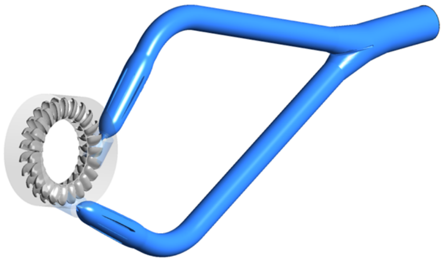

Simulazione dei getti e relativo dettaglio:

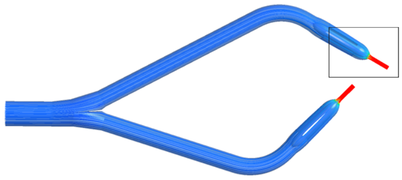

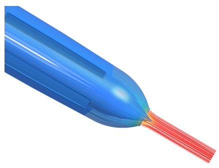

Turbina Pelton - 2

Dominio di calcolo e condizioni al contorno:

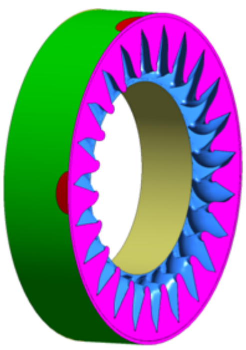

Boundary conditions:
Inlet - red
Outlet - green
Opening - yellow
Simmetry - magenta
Blue - wall

Dettagli della griglia all'ingresso e sulle superfici delle pale (buckets):

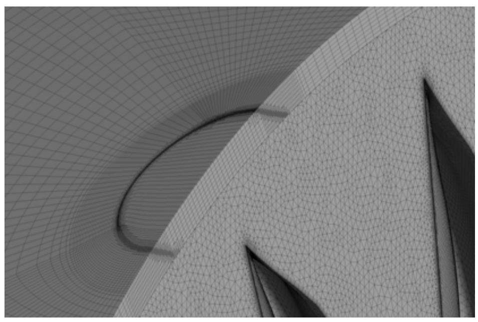

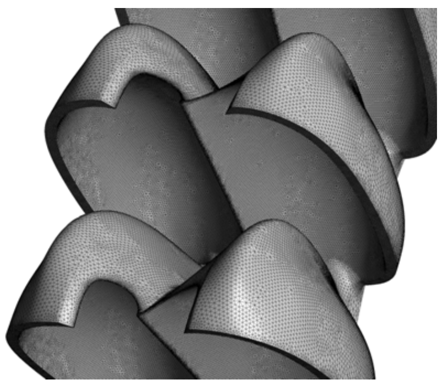

Turbina Pelton - 3

Coppia all'albero durante la simulazione:

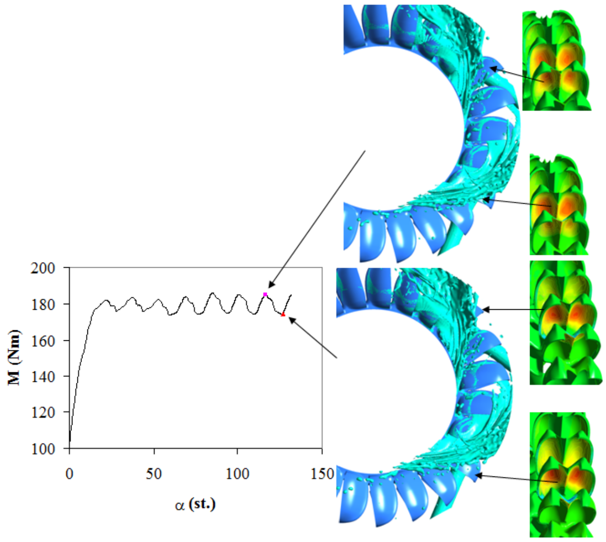

Flow pattern:

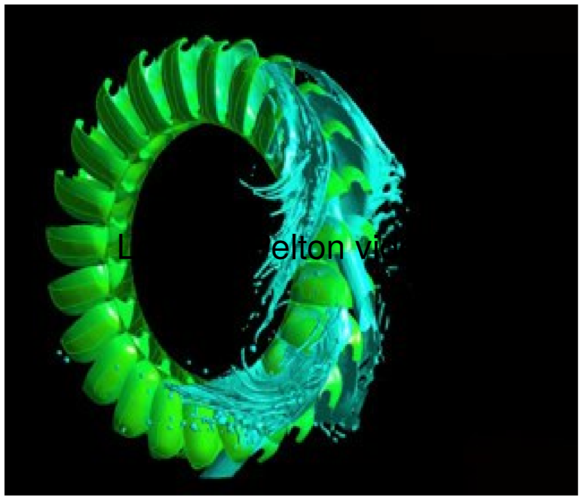

Turbina Pelton - 4

Efficienza calcolata e sperimentale:

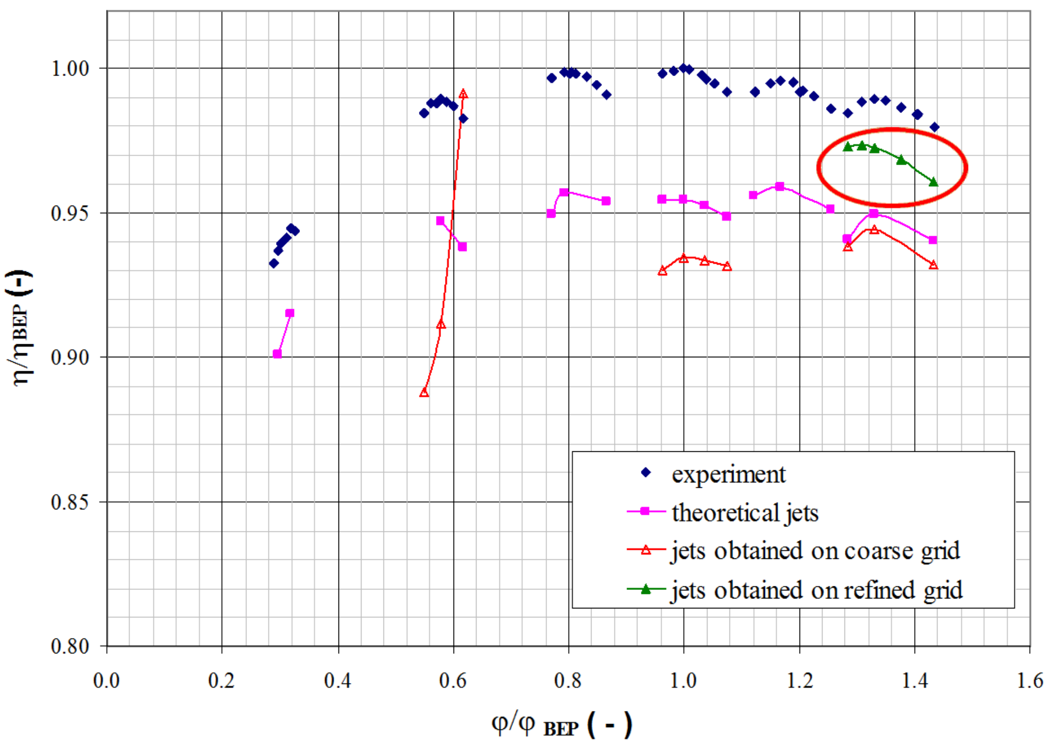

Lo stirring elettromagnetico

Analisi Numerica Multifisica di Agitatori Elettromagnetici Rotativi

Definizione

Mescolamento di un metallo liquido attraverso campi elettromagnetici rotanti.

Applicazioni

Processi di colata.

Benefici

- favorisce lo scambio termico;
- promuove la crescita di zone equiassiche durante il processo di solidificazione;
- favorisce la degassificazione e riduce le porosità;
- controlla la superficie libera dell'acciaio liquido in lingottiera limitando le inclusioni;

Miglioramento delle proprietà meccaniche degli acciai.

Stirrer

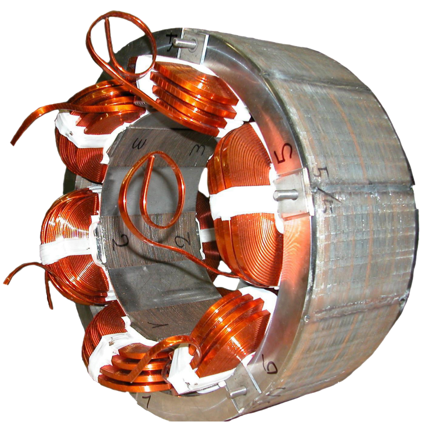

Principio di funzionamento:

- il campo rotante induce delle correnti nel metallo liquido;
- le cariche, immerse in un campo magnetico in moto relativo, sono soggette alla forza di Lorentz;
- il fluido viene messo in movimento.

Flussi secondari - 1

Il movimento rotatorio indotto dagli stirrer nel metallo liquido genera importanti moti secondari. Si considerino ora i due casi più importanti di stirring:

- Stirring all'interno di un recipiente (alluminio, leghe leggere);

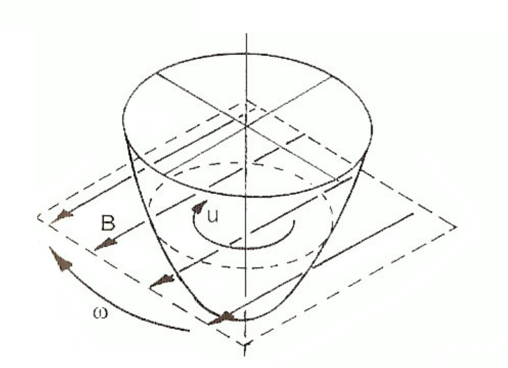

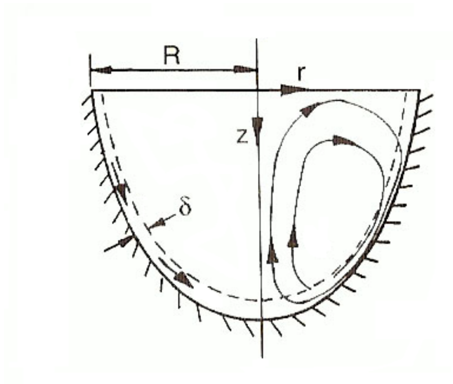

Flussi secondari - 2

- Stirring in lingottiera nei processi di colata continua.

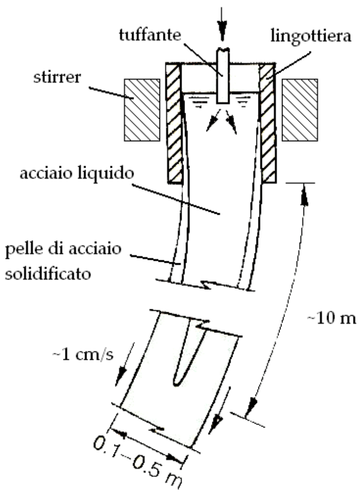

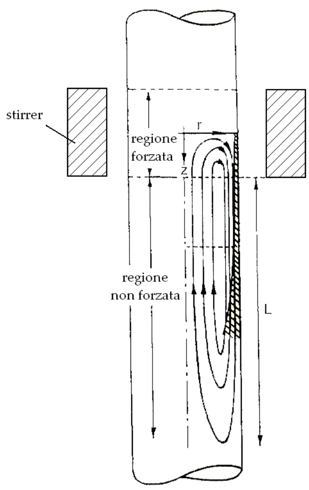

Le misure in lingottiera sono praticamente impossibili: necessario affidarsi a strumenti di simulazione al calcolatore.

Simulazioni elettromagnetiche

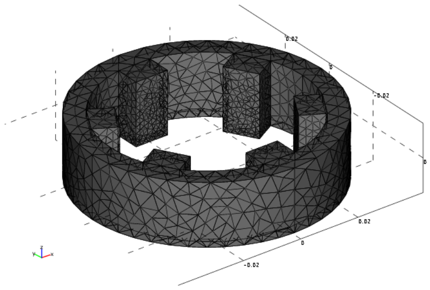

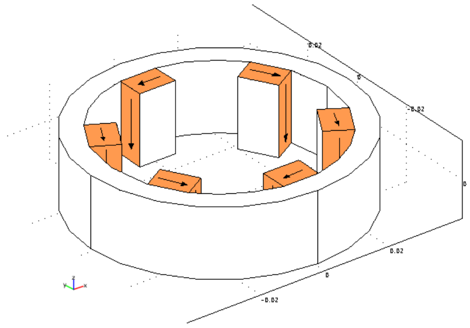

- L'anello dello stirrer e l'aria vengono considerati come corpi continui ed isotropi;
- Viene imposta la circolazione di correnti di superficie sulle facce delle scarpe per simulare gli avvolgimenti;
- Sulle facce dell'“universo” vengono settate le condizioni di isolante magnetico.

$$\left(j\omega\sigma + \omega^2\varepsilon_0\varepsilon_r\right)\mathbf{A} + \nabla\times\left(\mu_0^{-1}\mu_r^{-1}\nabla\times\mathbf{A}\right) = \mathbf{J}^e$$

Campo magnetico generato dagli stirrer

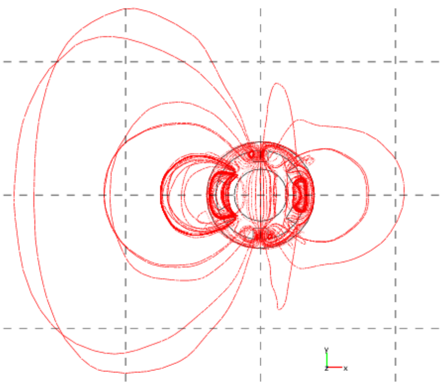

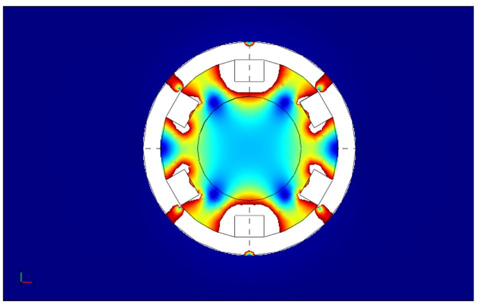

Campo in un istante:

$$B = (real(B_x)^2 + real(B_y)^2 + real(B_z)^2)^{1/2}$$

Campo mediato nel tempo:

$$B_{ave} = [0.5 \cdot real(B_x \cdot conj(B_x)) + 0.5 \cdot real(B_y \cdot conj(B_y)) + 0.5 \cdot real(B_z \cdot conj(B_z))]^{1/2}$$

Forze di Lorentz

Valore istantaneo:

$$F_x = real(Ji_y) \cdot real(B_z) - real(Ji_z) \cdot real(By)$$

$$F_y = real(Ji_z) \cdot real(B_x) - real(Ji_x) \cdot real(Bz)$$

$$F_z = real(Ji_x) \cdot real(B_y) - real(Ji_y) \cdot real(Bx)$$

Valore mediato nel tempo:

$$F_{x_{ave}} = 0.5 \cdot real(Ji_y \cdot conj(B_z) - Ji_z \cdot conj(B_y))$$

$$F_{y_{ave}} = 0.5 \cdot real(Ji_z \cdot conj(B_x) - Ji_x \cdot conj(B_z))$$

$$F_{z_{ave}} = 0.5 \cdot real(Ji_x \cdot conj(B_y) - Ji_y \cdot conj(B_x))$$

Forze indotte nell'acciaio

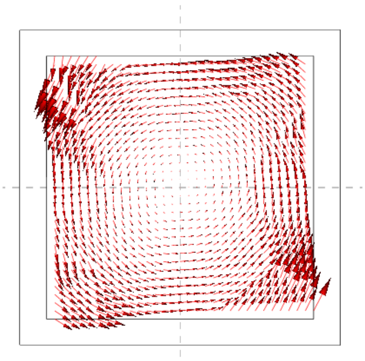

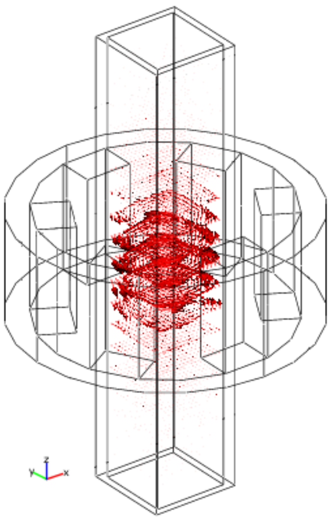

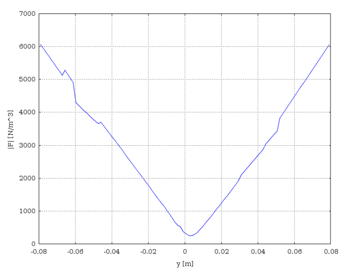

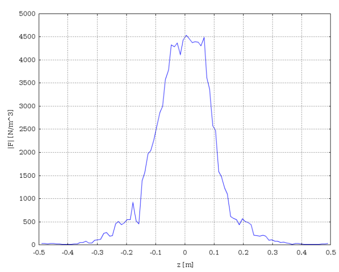

Campo di moto con tuffante

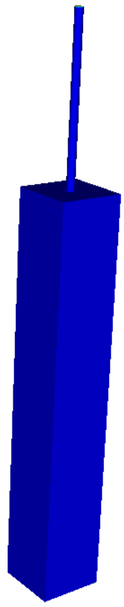

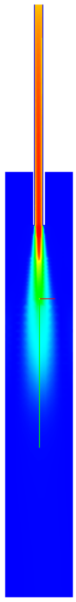

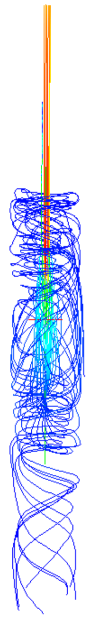

Introduction

Metal Foams

- Porous materials with low densities and tortuous and irregular flow passages
- Pore density 5-100 PPI, porosity 80-97%
- Good candidates for enhancing thermal performances of heat transfer devices

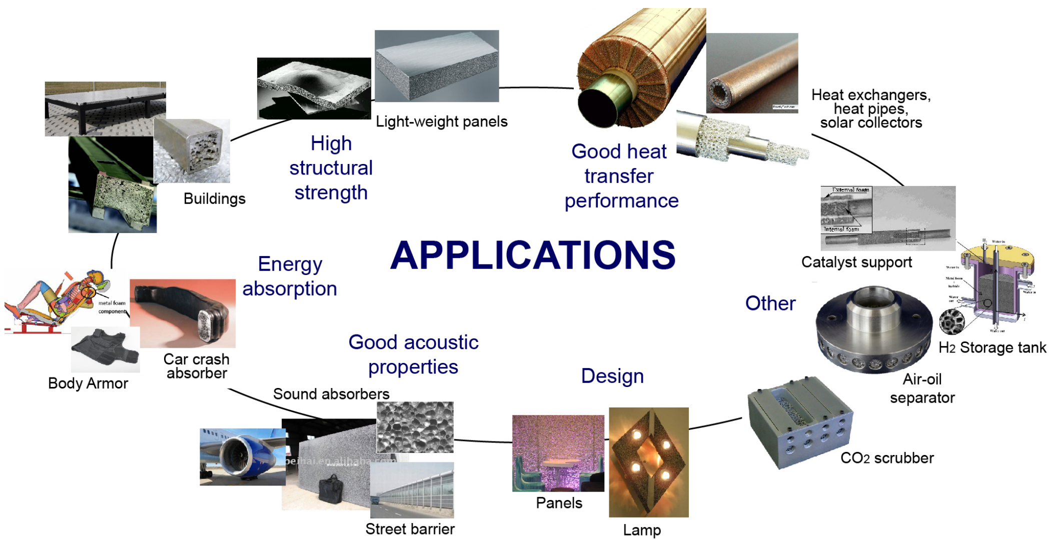

Introduction

Great potential for enhancing thermal performances due to:

- High surface area to volume ratio
- High conductivity of the solid ligaments
- Enhanced flow mixing $\longleftrightarrow$ tortuous and irregular flow passages

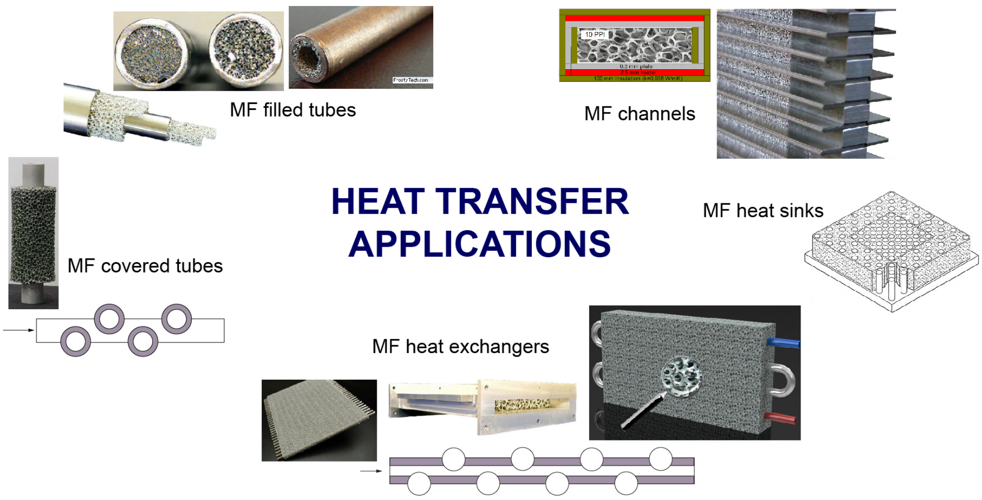

Approaches

For practical applications

It is necessary to characterize and quantify their transport and thermal properties: permeability, K, and effective thermal conductivity, k_{eff}.

- not simple
- information is sometimes scarce

Approaches

- Classical approaches
  - asymptotic solutions
  - empirical correlations
  - unit cell approaches
- CFD simulations
  - simplified models
  - realistic geometries

Many works about porous media, some of which specifically derived for metal foams.

Possible strategies for CFD simulations

- Macroscopic approach
  - Volume Averaging approach
  - the governing equations are volume averaged
  - the porous solid-fluid system is treated as a homogeneous medium
  - the small-scale details are neglected
- Microscopic approach (pore-based approach)
  - Representative Elementary Volume (REV) approach
  - the complex (real or idealized) geometry of the system is considered
  - the small-scale flow details are captured
  - potentially more accurate
  - more costly

REV (Representative Elementary Volume)

- The smallest control volume that gives statistically meaningful local average properties (porosity, permeability, ...)
- When appropriately chosen, addition of extra pores does not change the magnitude of these local properties.

Possible strategies for CFD simulations

Microscopic approach

The microscopic approach is necessary for the quantification of:

- the pressure drop
- the local heat transfer coefficient
- the effective thermal conductivity of the medium

Simplified domains

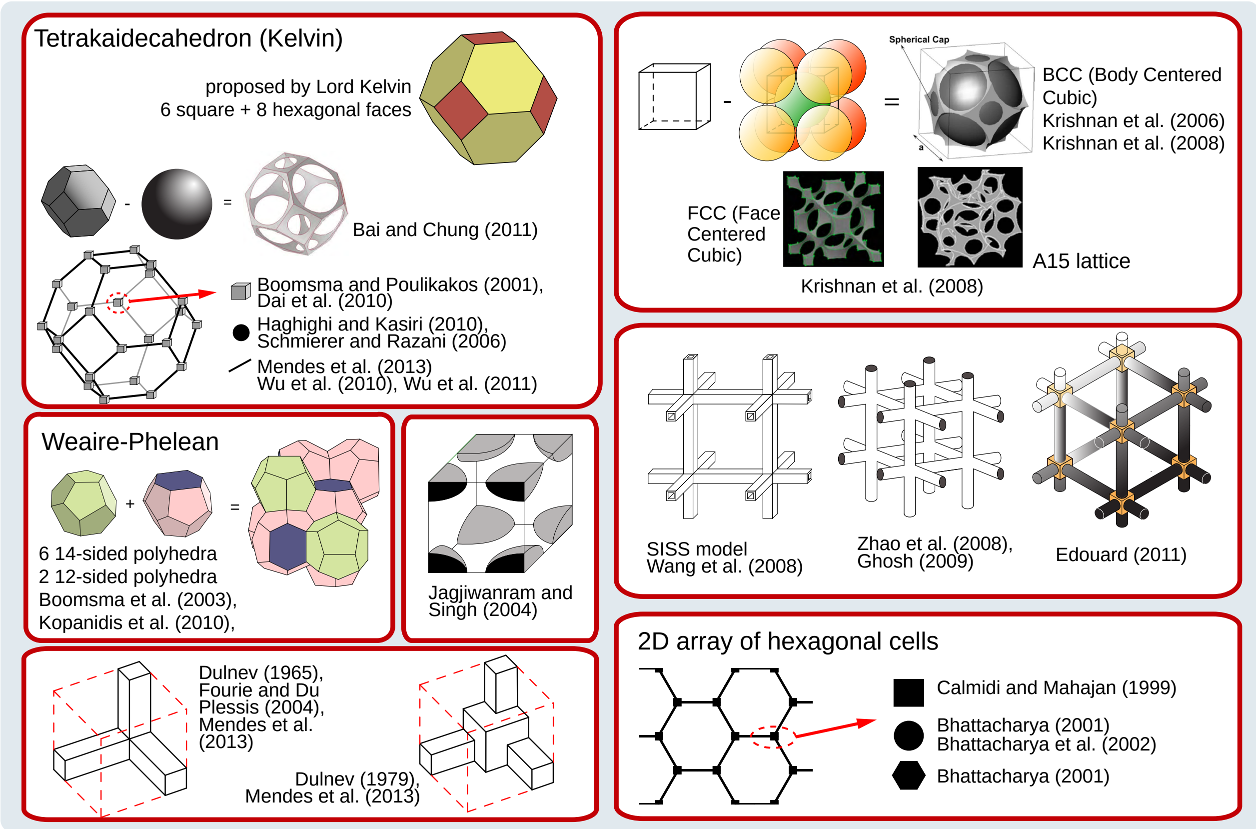

X-ray μ-CT

Non invasive X-ray based method allowing the 3D reconstruction of an opaque sample by illuminating it in different directions.

- An X-ray beam is sent on a sample and the transmitted beam is recorded on a detector
- The sample is made to rotate around its axis
- The total rotational angle depends on both the geometry of the sample and the beam: 180° for nearly parallel beam (e.g., synchrotron) or 360° for cone-beam

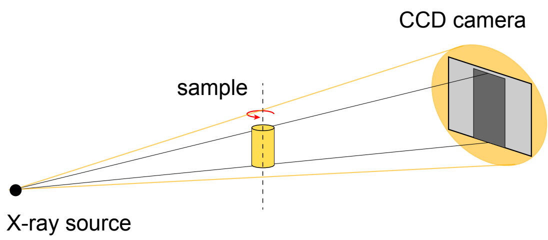

- Several radiographs are recorded at different angles, corresponding to the projection of the linear attenuation coefficient:

$$I = I_0 e^{-\alpha x} \qquad \text{Lambert-Beer Law}$$

I_0: incident intensity radiation intensity
I: emergent (transmitted) radiation intensity
α: linear attenuation coefficient of the material

x: thickness of the medium

- Attenuation depends on both the composition and density of the sample

- The volume can be reconstructed from the set of 2D radiographs with a suitable algorithm

Process

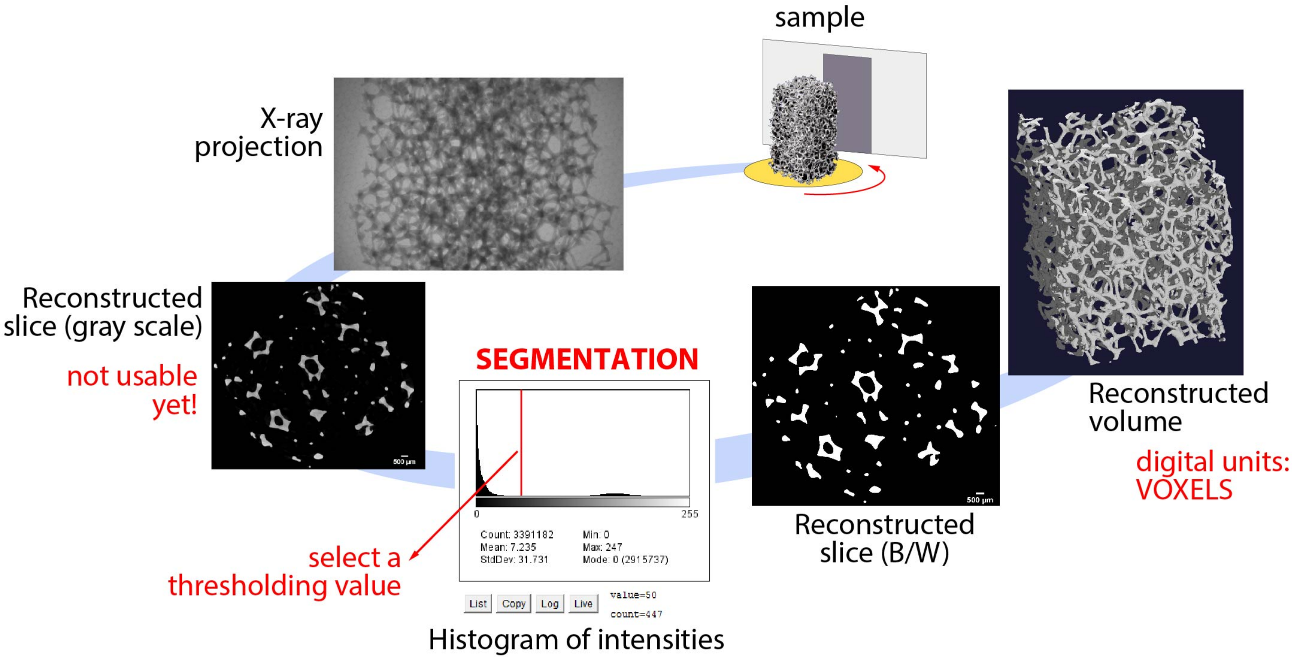

Effect of the threshold value

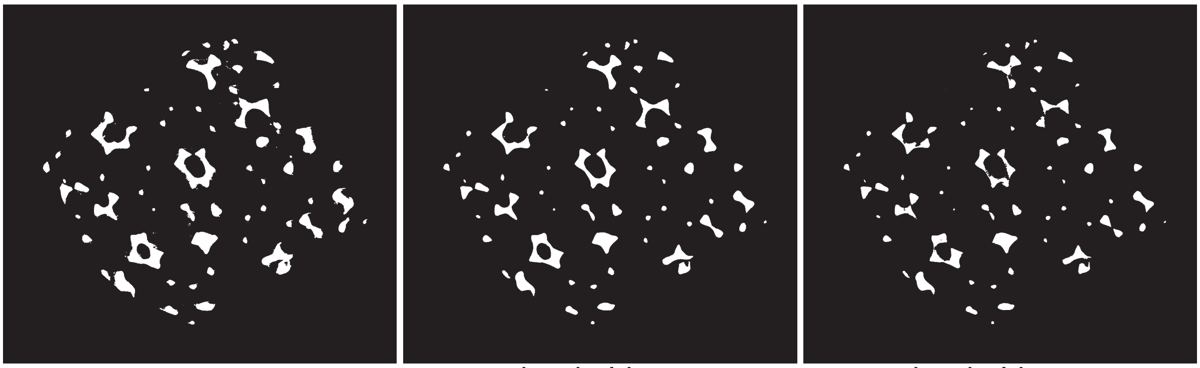

Threshold = 20 Threshold = 80 Threshold = 140

Synchrotron radiation

> *"Modern laboratory μ-CT setups based on conebeam geometry can produce high-resolution images and due to the small focal spot size of the source they also exhibit phase-contrast effects, but such effects are limited in comparison to synchrotron hard X-ray imaging beamlines."*
>
> Baker et al., Lithos 148 (2012) 262-276.

The use of synchrotron sources can improve significantly the image quality and reduce the scanning time.

- Characteristics:
  - monochromatic beam $\longrightarrow$ no beam hardening effects and high signal-to-noise ratio
  - nearly parallel beam geometry
- Advantages:
  - very high spatial resolutions, even at relatively large sample-to-detector distances
  - more precise definition of the scanned geometry
  - phase-contrast imaging and holotomography can be performed
- However, synchrotron μ-CT is not free of artifacts, e.g., ring artifacts.

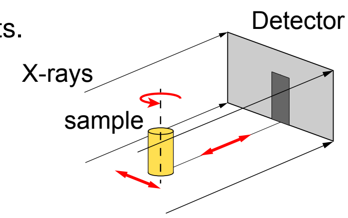

Aluminum foam samples

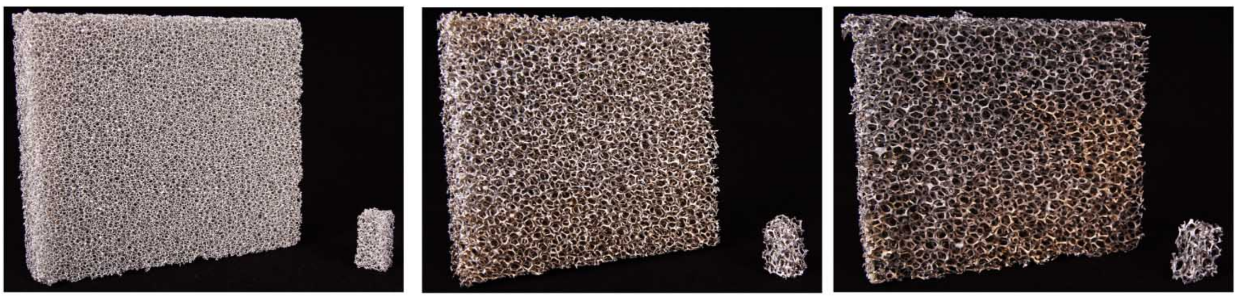

30 PPI 20 PPI 10 PPI

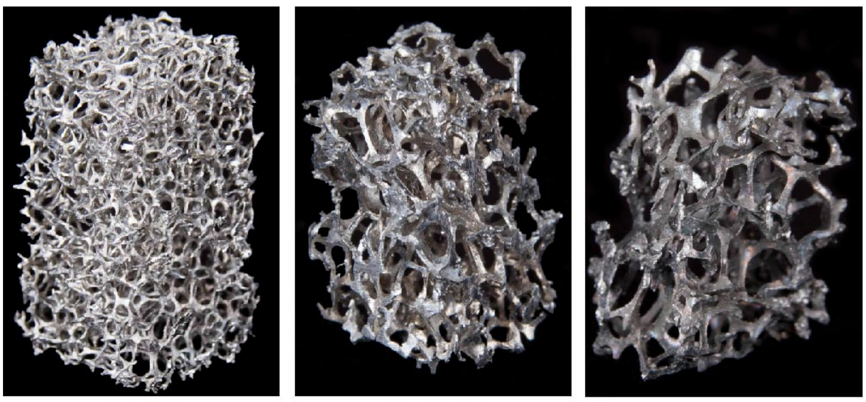

30 PPI 20 PPI 10 PPI

TomoLab Station c/o Elettra Synchrotron Radiation Facility (Trieste)

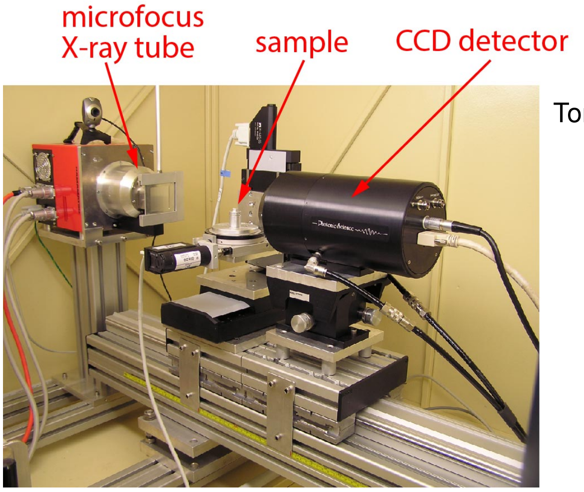

TomoLab Station:

- cone-beam tomographic system
- minimum focal spot size: 5 μm
- energy range 40-130 kV
- maximum current 300 A
- water-cooled 12 bit CCD camera (4008×2672 pixels, effective pixel size $12.5 \times 12.5 \mu m^2$)

Experimental conditions:

- voltage: 60 kV, current: 133 μA
- number of recorded projections: 2400 (time: 2h30')
- rotation: 360°
- source-to-sample distance: 80 mm
- source-to-detector distance: 220 mm
- 0.5 mm thick Al filter

Absorption μ-CT at 9.1 μm resolution.

http://www.elettra.trieste.it/lightsources/labs-and-services/tomolab/tomolab.html

Reconstructed volumes

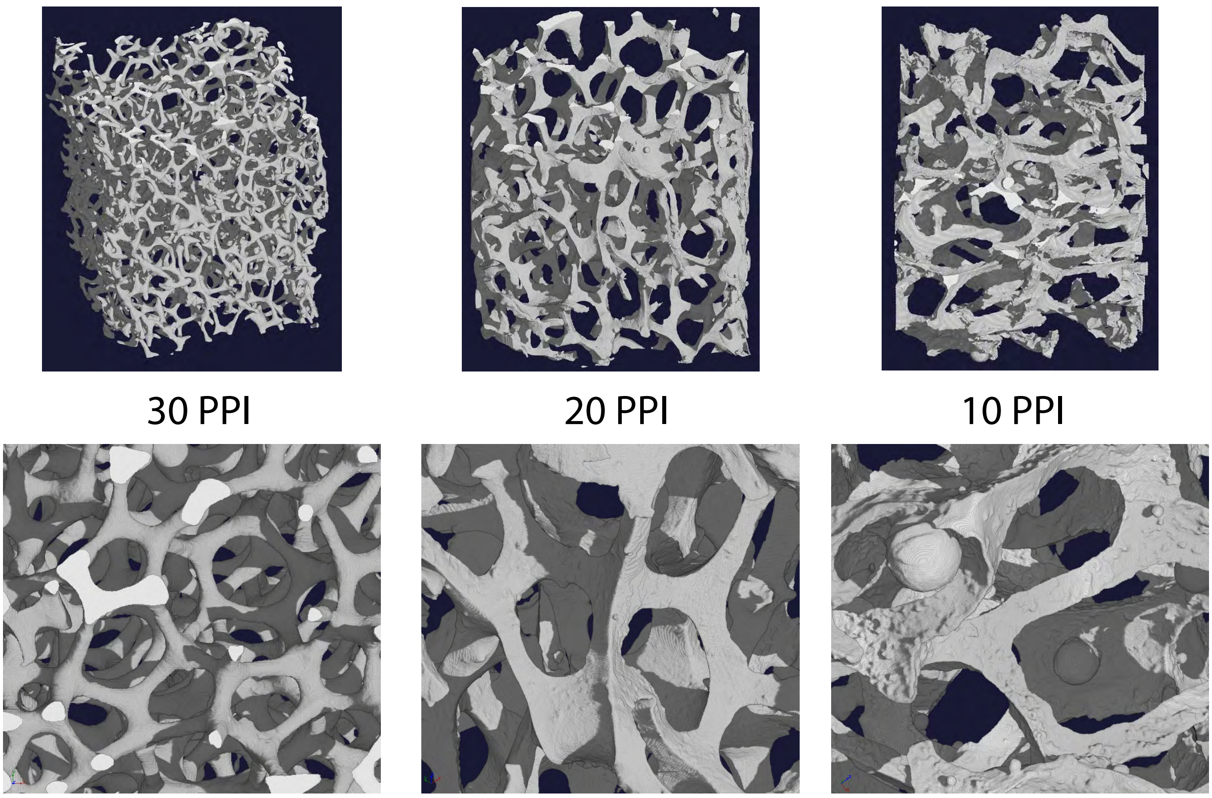

Reconstructed volumes - cont.

The superficial characteristics of the foams vary according to the PPI:

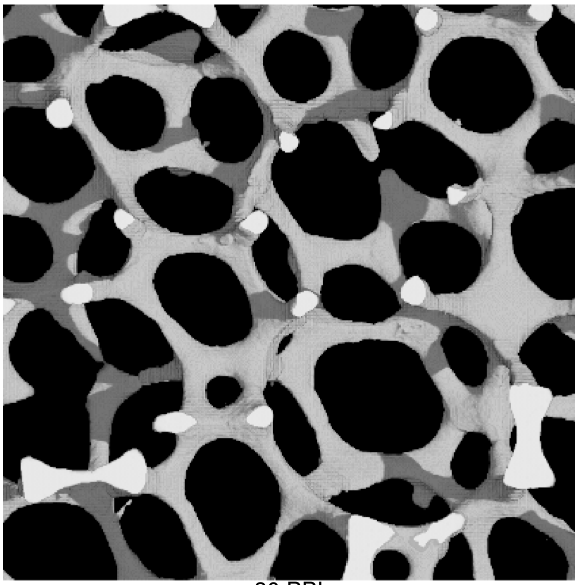

30 PPI

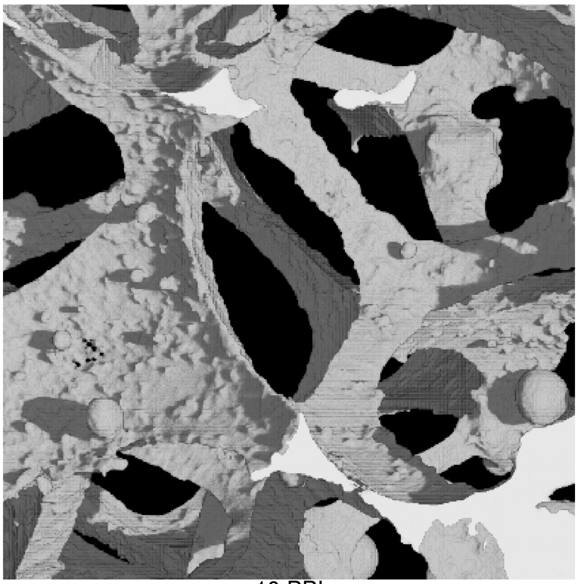

10 PPI

Surface triangulation

- At this point it is necessary to generate a .stl file of the geometry, to be used in the following meshing stage
- VGStudio MAX 2.0 (Volume Graphics)
- In order to generate a usable geometry file, the surface of the mesh must be triangulated

Note

A compromise must be done between:

- accuracy of the triangulation
- size of the exported file

Too heavy files are problematic to handle in the next meshing stage!

↓

This stage introduces an approximation in the process.

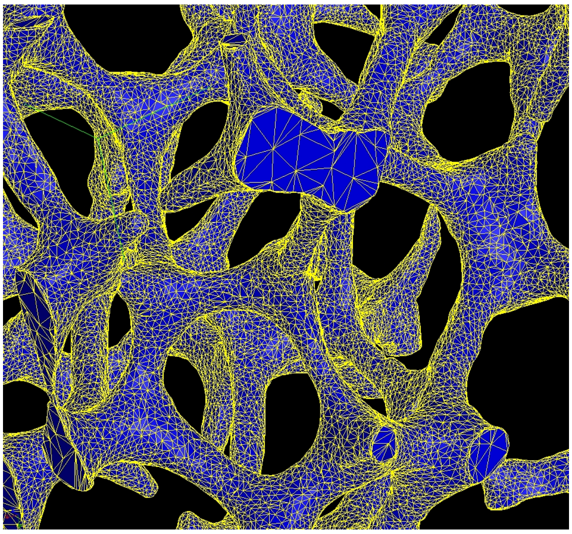

http://www.volumegraphics.com/en/products/vgstudio-max.html

Domains

From each reconstructed volume, a smaller representative cubic volume element was extracted:

- 30 PPI: 548^3 voxels
- 20 PPI: 848^3 voxels
- 10 PPI: 1000^3 voxels

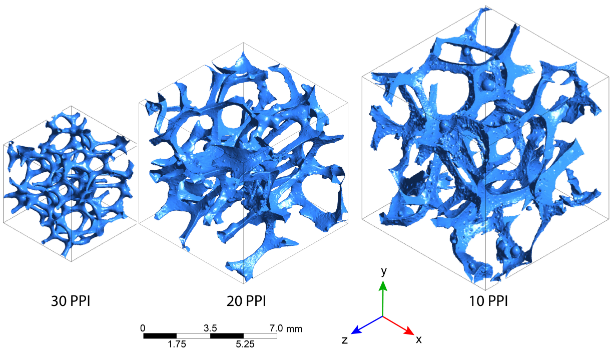

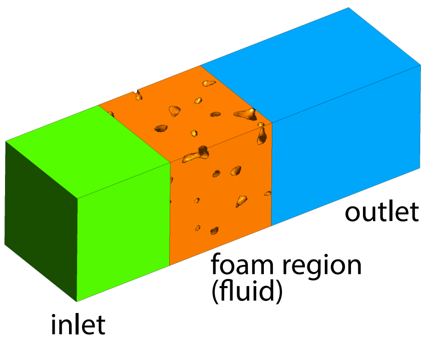

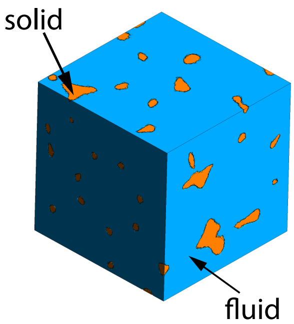

Meshing

- Mesh: geometrically exact, feature-preserving grids
  - central foam region: tetrahedral elements
  - inlet and outlet regions: orthogonal hexahedral mesh
- ANSYS ICEM CFD
- Number of nodes:
  - Flow + Heat transfer (central foam region):
    - 30 PPI: ~1.4×10^6 nodes
    - 20 PPI: ~2.4×10^6 nodes
    - 10 PPI: ~4.1×10^6 nodes
  - Thermal conductivity:
    - 30 PPI: solid ~0.54×10^6, fluid ~0.63×10^6 nodes
    - 20 PPI: solid ~0.83×10^6, fluid ~0.52×10^6 nodes
    - 10 PPI: solid ~1.00×10^6, fluid ~0.65×10^6 nodes

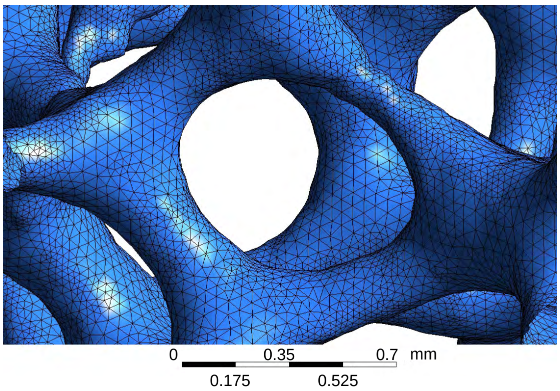

30 PPI

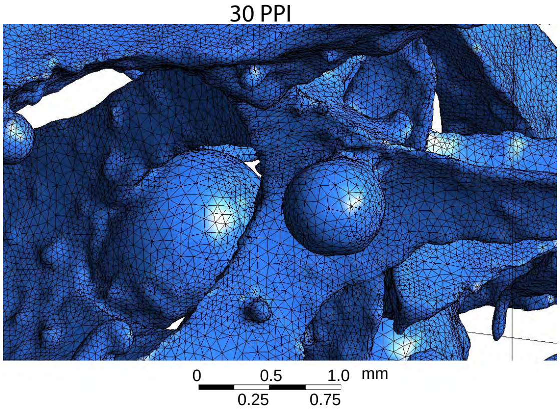

10 PPI

Meshing - cont.

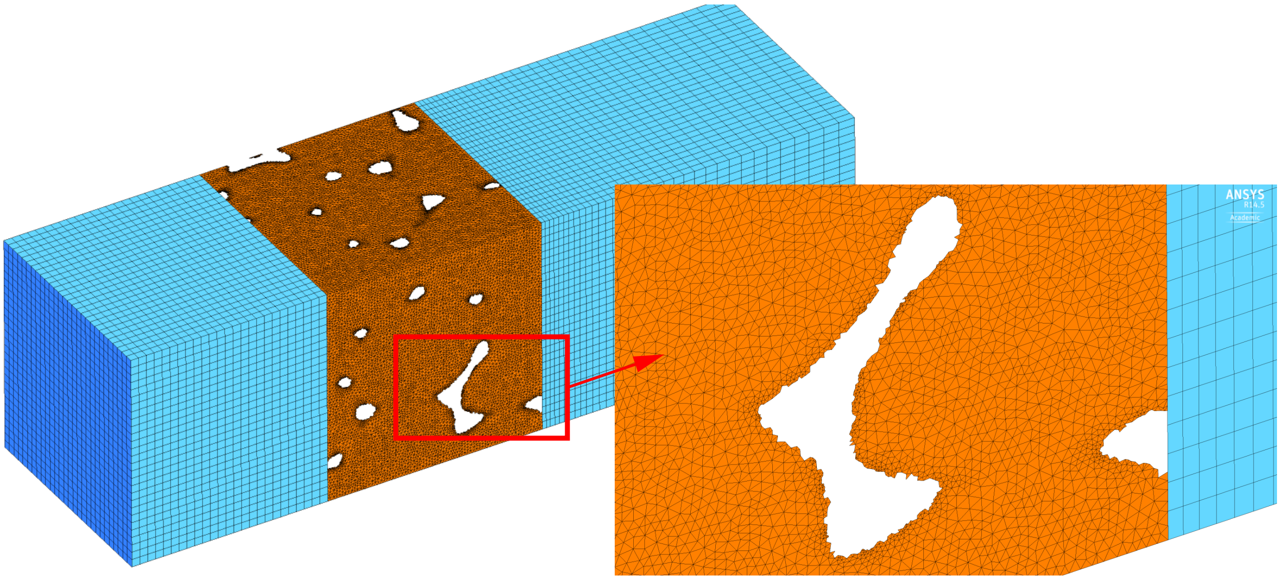

30 PPI

Meshing

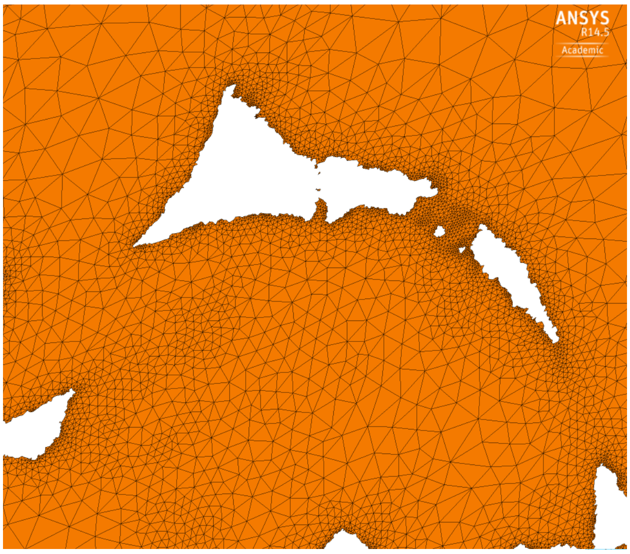

10 PPI

30 PPI

Computational domains

Flow + Heat transfer

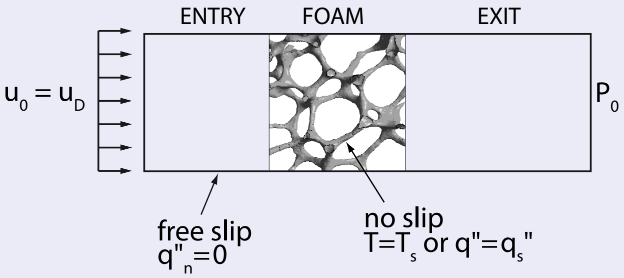

- Air with constant thermophysical properties at 25 °C
- laminar: $Re_p = 1 \div 200$
- steady flow regime
- simulations performed along the three space directions

Thermal conductivity

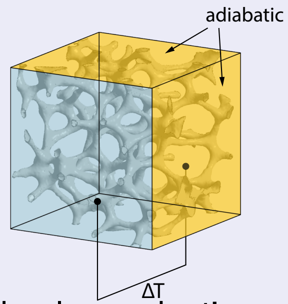

- Solved only conduction equation (no fluid motion), both in the fluid and in the solid, simultaneously
- A fixed (arbitrary) $\Delta T = 10$K set across the domain
- Other faces kept adiabatic
- Both air and water simulated
- k_{eff} estimated along the three space directions

The flow field

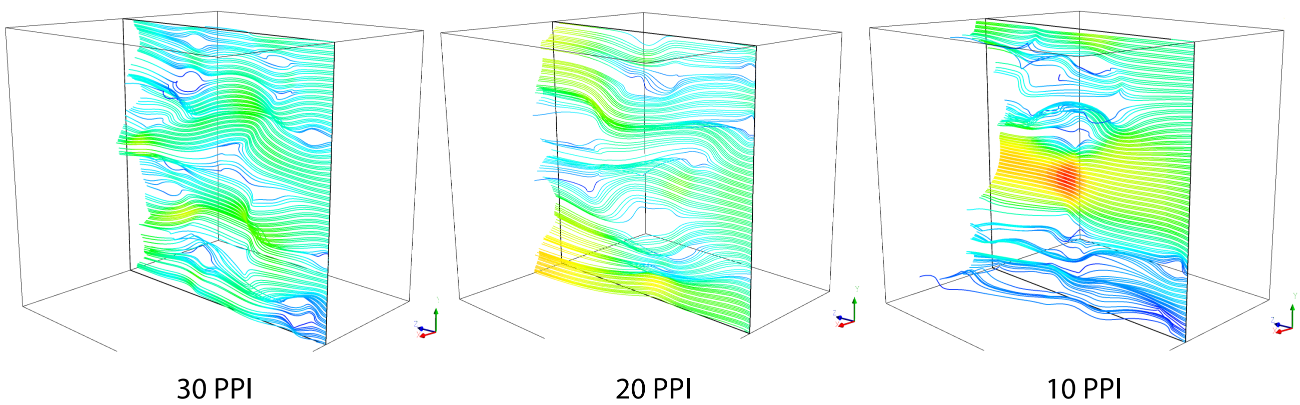

Figura: Flow streamlines at $Re = 10$.

The flow field

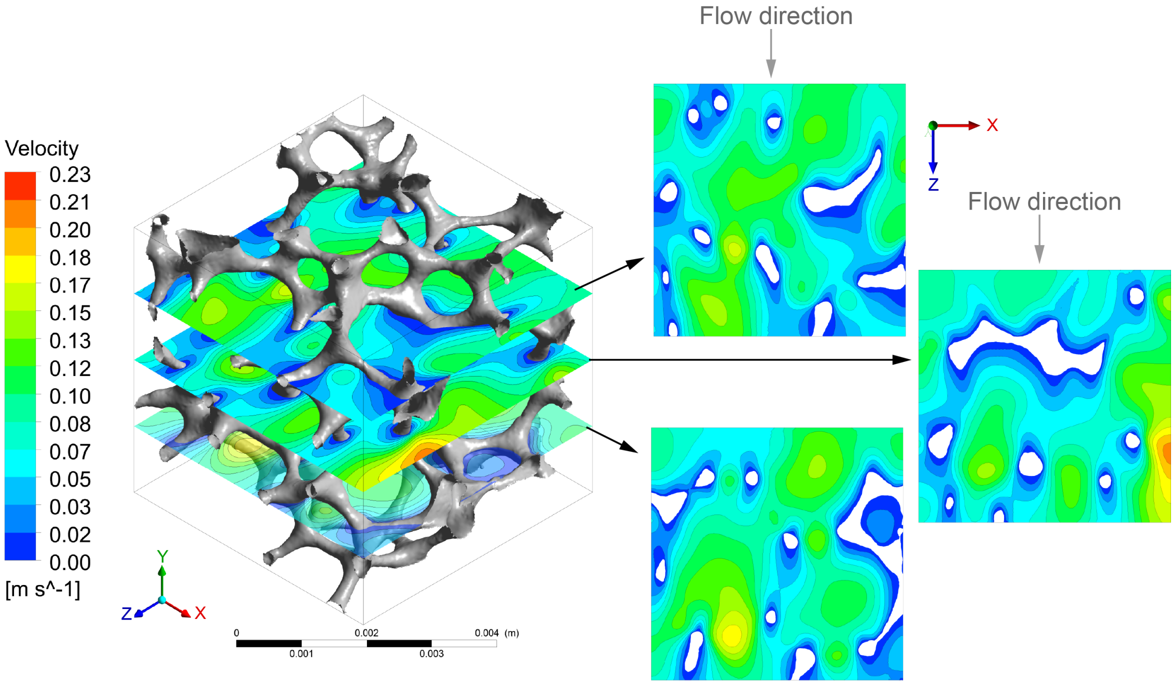

Figura: Visualization of the velocity contours inside the 30 PPI foam at three different sections.

Permeability

$$\frac{\nabla P \cdot d_p^2}{\mu \cdot u_D} = -\frac{d_p^2}{K} - C d_p Re$$

	30 PPI		20 PPI		10 PPI	
	$\varepsilon = 0.929$		$\varepsilon = 0.935$		$\varepsilon = 0.944$	
	$K \times 10^7$	C	$K \times 10^7$	C	$K \times 10^7$	C
x	0.872	389.0	2.694	240.3	2.906	218.6
y	0.859	392.9	2.342	250.3	3.058	255.2
z	0.858	370.6	2.306	257.6	3.234	187.9
Av.	0.863	384.2	2.477	249.4	3.066	220.6

Tabella: Values of permeability K [m^2] and of the Dupuit-Forchheimer coefficient C [m^{-1}], for the three foam samples. $Av.$ refers to the value averaged along the three directions. ε is the porosity of the foam.

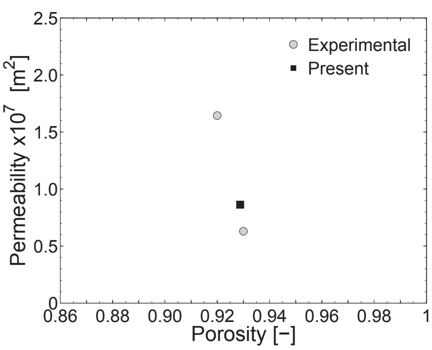

30 PPI

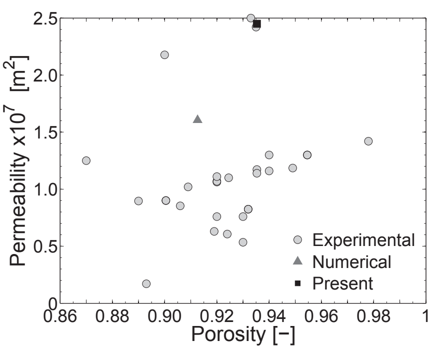

20 PPI

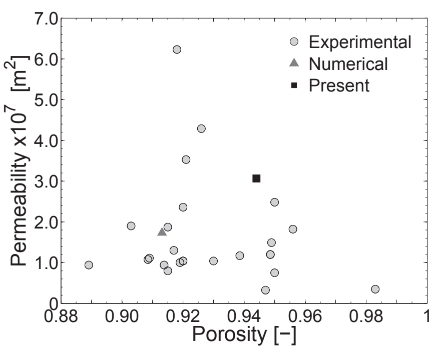

10 PPI

Effective thermal conductivity

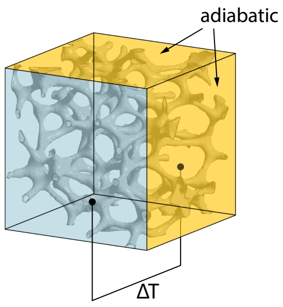

- Solved only conduction equation (no fluid motion), both in the fluid and in the solid, simultaneously
- A fixed (arbitrary) $\Delta T = 10$K set across the domain
- Other faces kept adiabatic
- Both air and water simulated
- k_{eff} estimated along the three space directions

$$k_{\text{eff}} = \frac{-\int \mathbf{J}\cdot d\mathbf{A}}{\frac{\partial T}{\partial x_i} A} = \frac{-\left(\int_s \mathbf{J}\cdot d\mathbf{A}_s + \int_s \mathbf{J}\cdot d\mathbf{A}_f\right)}{\frac{\partial T}{\partial x_i}\left(A_s + A_f\right)}$$

$\mathbf{J}$: heat flux
$d\mathbf{A}$: outward pointing area vector
s: refers to the solid
f: refers to the fluid

Results

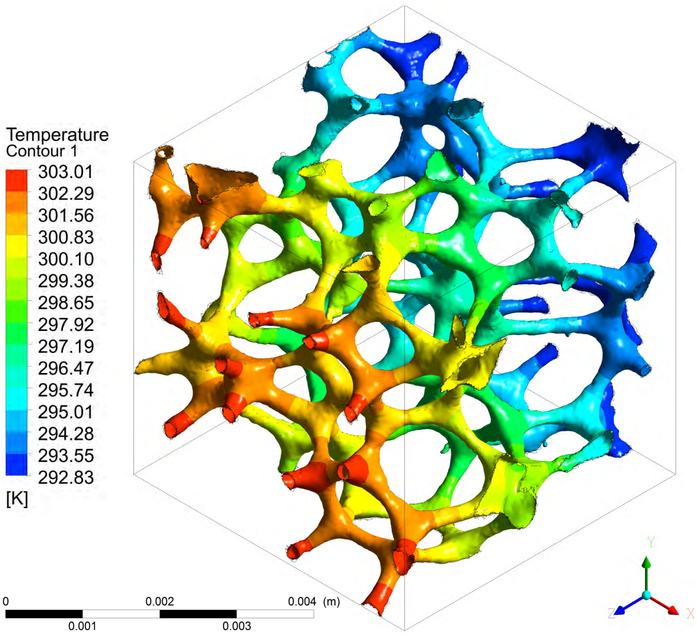

Figura: 30 PPI, temperature gradient applied along the z direction.

Results

PPI	Porosity	air	water
10	0.944	3.49	4.13
20	0.927	4.57	5.27
30	0.929	5.31	5.99

- k_{eff} with water is slightly larger than that with air
- the thermal conductivity of the fluid influences, but not in a significant way, k_{eff}

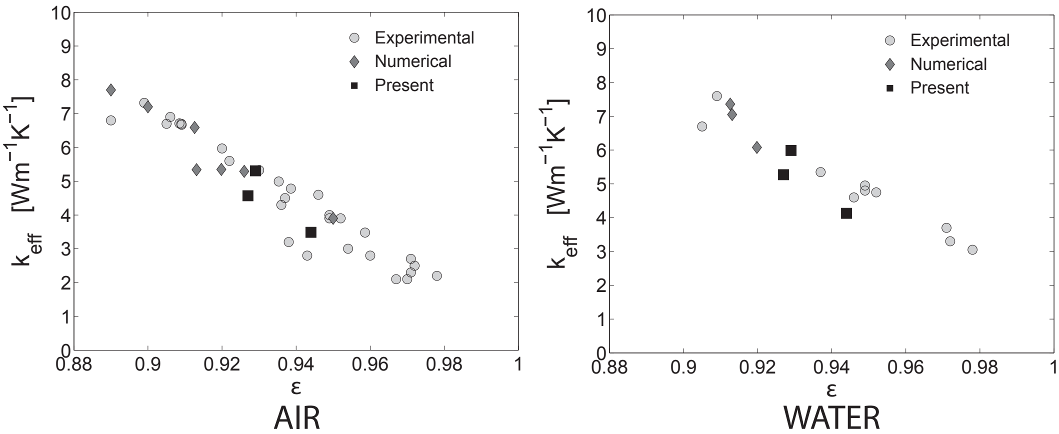

Example of application

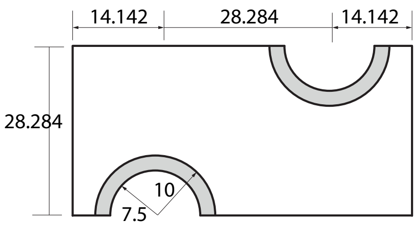

Porosity	ε	0.929
Permeability	K	8.631×10^{-6} m^2
Form drag coefficient	C	384.2×10^3 m^{-1}
Effective thermal conductivity	k_{eff}	W/(m K)

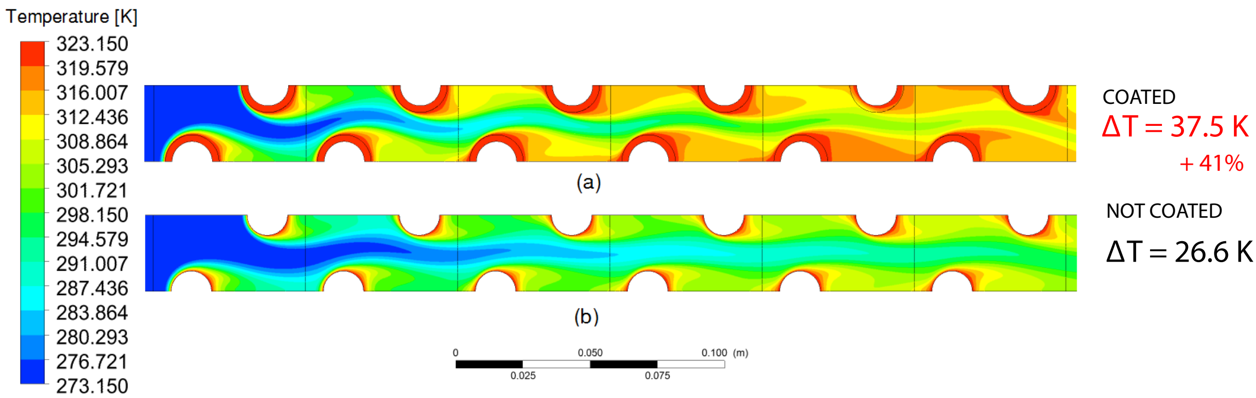

Example of application

The heat transfer enhancement is gained at the expense of a triple pressure loss

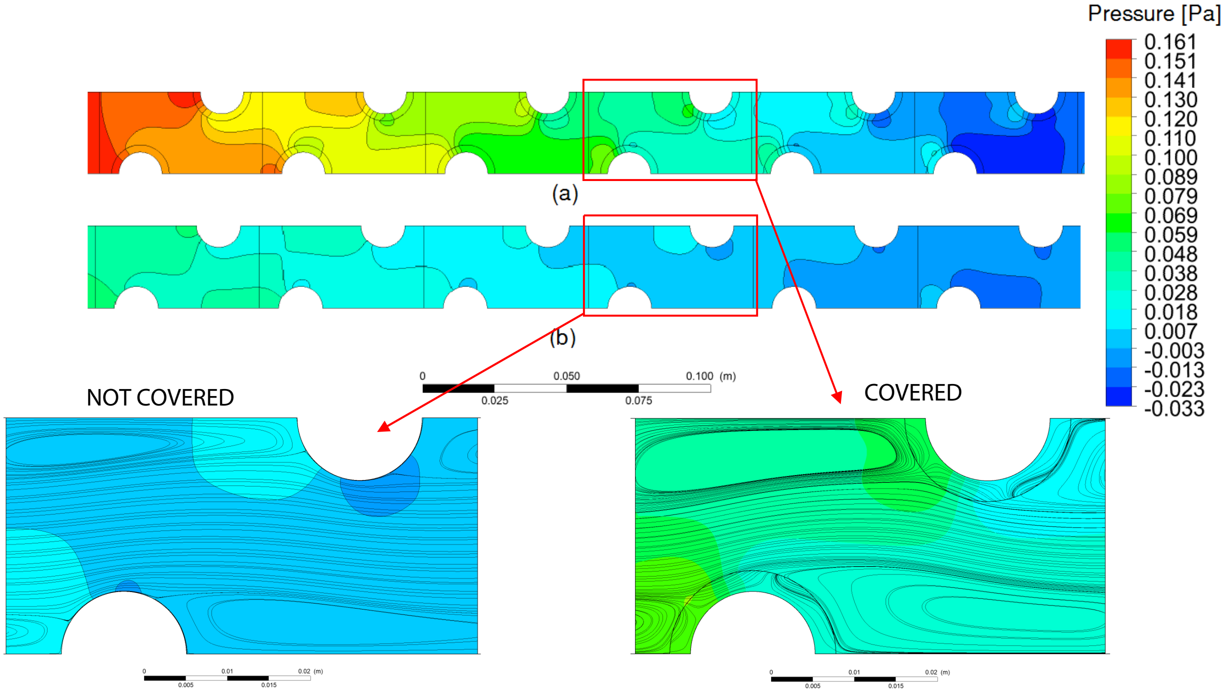

Incendi e fumi

Per gentile concessione M. Manzan

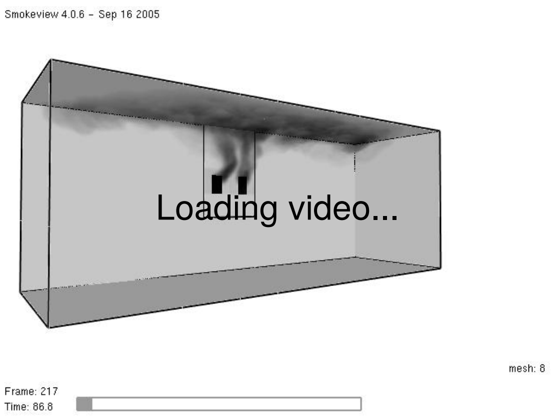

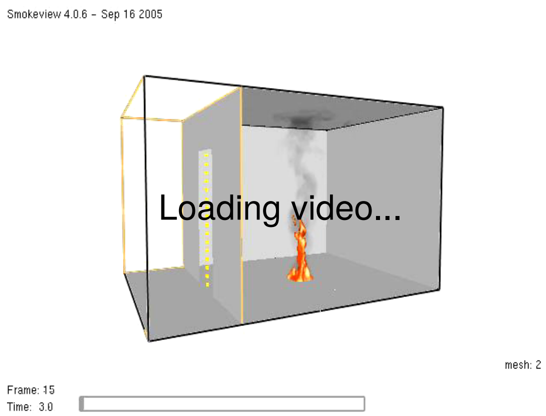

CFD nella medicina Cardiovascolare

Review

Computational fluid dynamics modelling in cardiovascular medicine

OPEN ACCESS

Paul D Morris,[1,2,3] Andrew Narracott,[1,2] Hendrik von Tengg-Kobligk,[4] Daniel Alejandro Silva Soto,[1,2] Sarah Hsiao,[1] Angela Lungu,[1,2] Paul Evans,[1,2] Neil W Bressloff,[5] Patricia V Lawford,[1,2] D Rodney Hose,[1,2] Julian P Gunn[1,2,3]

▸ Additional material is published online. To view please visit the journal (http://dx.doi.org/10.1136/heartjnl-2015-308044)

[1]Department of Cardiovascular Science, University of Sheffield, Sheffield, UK
[2]Insigneo Institute for In Silico Medicine, Sheffield, UK
[3]Department of Cardiology, Sheffield Teaching Hospitals NHS Trust, Sheffield, UK
[4]University Institute for Diagnostic, Interventional and Pediatric Radiology, University Hospital of Bern, Inselspital, Bern, Switzerland
[5]Faculty of Engineering & the Environment, University of Southampton, Southampton, UK

Correspondence to
Dr Paul D Morris, Medical Physics Group, Department of Cardiovascular Science, University of Sheffield, The Medical School, Beech Hill Road, Sheffield S102RX, UK; paulmorris@doctors.org.uk

Received 23 April 2015
Revised 20 September 2015
Accepted 21 September 2015
Published Online First 28 October 2015

Open Access
Scan to access more free content

CrossMark

To cite: Morris PD, Narracott A, von Tengg-Kobligk H, *et al. Heart* 2016;**102**:18–28.

ABSTRACT

This paper reviews the methods, benefits and challenges associated with the adoption and translation of computational fluid dynamics (CFD) modelling within cardiovascular medicine. CFD, a specialist area of mathematics and a branch of fluid mechanics, is used routinely in a diverse range of safety-critical engineering systems, which increasingly is being applied to the cardiovascular system. By facilitating rapid, economical, low-risk prototyping, CFD modelling has already revolutionised research and development of devices such as stents, valve prostheses, and ventricular assist devices. Combined with cardiovascular imaging, CFD simulation enables detailed characterisation of complex physiological pressure and flow fields and the computation of metrics which cannot be directly measured, for example, wall shear stress. CFD models are now being translated into clinical tools for physicians to use across the spectrum of coronary, valvular, congenital, myocardial and peripheral vascular diseases. CFD modelling is apposite for minimally-invasive patient assessment. Patient-specific (incorporating data unique to the individual) and multi-scale (combining models of different length- and time-scales) modelling enables individualised risk prediction and virtual treatment planning. This represents a significant departure from traditional dependence upon registry-based, population-averaged data. Model integration is progressively moving towards 'digital patient' or 'virtual physiological human' representations. When combined with population-scale numerical models, these models have the potential to reduce the cost, time and risk associated with clinical trials. The adoption of CFD modelling signals a new era in cardiovascular medicine. While potentially highly beneficial, a number of academic and commercial groups are addressing the associated methodological, regulatory, education- and service-related challenges.

INTRODUCTION

Computational fluid dynamics (CFD) is a well-established tool used in engineering, in many areas of which it has become the primary method for design and analysis. Bioengineers have adopted CFD to study complex physiological flows and have demonstrated their potential.[1] There is increasing interest in applying these methods in cardiovascular medicine.[2 3] CFD-based techniques are being used to build complex computer representations (in silico models) of the cardiovascular system in health and disease. CFD modelling is a new field within cardiovascular medicine, enhancing diagnostic assessment, device design and clinical trials. It can predict physiological responses to intervention and compute previously unmeasurable haemodynamic parameters.[4] As CFD modelling continues to translate into clinical tools, it is important that clinicians understand the principles, benefits and limitations of these techniques. This article explores these topics using state-of-the-art examples in key clinical areas, highlighting applications likely to impact clinical practice within the next 5 years (table 1).

WHAT IS CFD?

CFD is a specialist area of mathematics and a branch of fluid mechanics. It is used in the design of many safety-critical systems, including aircraft and vehicles, by solving differential equations to simulate fluid flow. A glossary of uesful terms is provided in table 2.

For incompressible flows, almost all CFD analyses solve the Navier-Stokes and continuity equations which govern fluid motion. These equations are non-linear, partial differential equations based upon the principle of conservation of mass and momentum. Simplification of these equations yields familiar formulae (eg, those of Bernoulli and Poiseuille); but for complex geometries analytical solutions are not possible, so specialised software applications (CFD solvers) calculate approximate numerical solutions. Non-linearity, due to convective fluid acceleration, makes this challenging, especially in three dimensional (3D) models; so CFD analyses require significant computational power and time.

CFD MODEL COMPLEXITY

The applications reviewed in this paper focus on 3D CFD analyses of local regions of the vasculature because this is where promising applications are beginning to translate and impact upon clinical medicine. There is a long history of simplification of the governing equations to lower spatial dimensions. Table 3 summarises the relationship between these approaches and provides clinical examples of their use.

2D analyses typically assume symmetry of the solution about the central axis, 1D models capture variation of the solution along the axial direction only, and 0D representations lump the behaviour of vascular regions into a model with no spatial dimensions, hence the term 'lumped-parameter models'. Due to the breadth of the literature covering application of these techniques to cardiovascular haemodynamics, the interested reader is referred to recent reviews of the state-of-the-art.[45 46]

CFD nella medicina Cardiovascolare - cont.

Review

Table 1 Summary of CFD modelling applications in cardiovascular medicine

Area	Clinical applications	Data and evidence	Potential clinical impact	Limitations and challenges	References
Coronary artery disease and physiology	Models based upon coronary angiography (CT /invasive) to compute physiological coronary lesion significance less invasively	Multiple trials demonstrating broadly good agreement between standard and CFD-derived FFR (vFFR). Lesion significance established in ~80–90%	Widened access to the benefits of physiological lesion assessment; vFFR lacks the practical limitations that restrict use of the invasive technique. Virtual stenting enables planning and selection of optimal treatment strategy	Accurate vessel reconstruction and patient-specific tuning of the model boundary conditions (especially those of myocardial resistance)	5 6 7 8
Valve prostheses	Evaluation and optimisation of prosthetic valve design from a haemodynamic perspective	Included in the design dossier given to RA for approval before use in humans. Third party, comparative studies are in engineering literature	CFD modelling enables the best design, yielding the optimal haemodynamics and lowest achievable risk of design-related thrombosis and thromboembolism	Dependence upon validity of models to interpret fluid stresses in terms of thrombogenic/haemolytic potential. Primarily relates to mechanical valves. Tissue valve leaflets remain challenging to model	9 10 11
Native valve haemodynamics in health and disease	Non-invasive computation and quantification of trans-valvular pressure drop and regurgitant fraction from CT imaging	Accurate 3D simulations in patient-specific models with valves in open and closed states to predict transvalvular dynamics in diseased states	Improved objective assessment and surveillance of valve disease from non-invasive imaging data	Requires high quality 3D images of valve orifice—not routinely generated. Balancing the requirement for complex dynamic simulation (FSI) vs simpler models (valve open/closed)	12 13
Aortic aneurysm	Provides quantitative haemodynamic data for non-invasive imaging to emphasise the significance of findings. Virtual therapy simulation/predictions	No published outcome trials, only single centre experiences and small cohorts using different boundary condition and computational methods	To better predict aneurysm progression and risk of rupture. Prediction of putative therapeutic effects. Individualised care and reduction in costs for unnecessary follow-up imaging and visits	Impact of low image contrast structures of aortic aneurysm (eg, wall, thrombus) as well as wall motion needs to be further assessed. CFD alone is probably limited and needs to be complemented by, for example, FSI	3 14 15 16
Aortic dissection	Pathophysiological conditions in true and false lumen computed from non-invasive boundary conditions (CT and MRI +PC). Effects of virtual therapy.	No published outcome trials, only single centre experiences and small cohorts using different boundary conditions and computational methods	Computed pressure and flow conditions used to guide (semi-) invasive therapeutic procedure decisions. Physiological effects of therapies can be simulated and better predicted	Significant early and late re-modelling of the dissected wall. Entry, re-entry and communication channels create a complex computational scenario. CFD alone might be limited. A potential role for FSI	17 18 19
Stent design	Prediction of WSS and related metrics that influence endothelial function and NH due to stent-induced haemodynamic disturbance	Turbulent or disturbed laminar flow reduces WSS stimulating adverse vessel remodelling. NH preferentially accumulates in these regions	Not possible to measure arterial WSS in vivo, especially in the vicinity of stent struts post-PCI. Modelling provides detailed analysis of flow, and the influence of stent design through patient-specific reconstructions, enabling the optimal stent design to be achieved	High resolution imaging, vessel reconstruction and boundary conditions are challenging. CFD simulations demand fine computational meshes and time-resolved pulsatility. Run-times are long, even with high performance computing	20 21 22 23 24 25 26 27
Cerebral aneurysm	Prediction of intra-aneurysmal flow, stasis, jet impingement and WSS from MRI and CT cerebral angiography data	Published data on association between WSS, aneurysm initiation, growth, and potentially rupture	Detailed, individualised haemodynamic analysis with potential for risk prediction. Impact of putative treatments on local haemodynamics evaluated in silico	Difficulty interpreting complex and detailed WSS results. Understanding how results translate to rupture risk. Validation of rupture predictions—a rare event	4 28 29
Pulmonary hypertension (PH)	Greater insights into complex PH physiology. Increasing interest in non-invasive diagnosis and monitoring of response to treatment	Models based on MR flows demonstrated to differentiate between healthy volunteers and to stratify PH subcategories	Imaging-based modelling of pulmonary haemodynamics can reduce the requirement for right heart catheterisation. Models show association between reduced WSS and invasive PH metrics. PH subtype characteristics simulated to understand the structural changes contributing to increased PAP	Spatial resolution of imaging and segmentation protocols. The use of a pressure surrogate measure. The presence of many outlets requiring many measurements to tune the outflow boundary conditions	30 31 32 33
Arterial wall shear stress (WSS)	WSS mapping, cross-referenced with	An abnormal WSS pattern has been correlated with	Ultimate understanding of the development and	A detailed vascular geometry is essential for an accurate	20 21 22 25

Continued

CFD nella medicina Cardiovascolare - cont

Review

Table 1 Continued

Area	Clinical applications	Data and evidence	Potential clinical impact	Limitations and challenges	References
	vascular disease phenotype, is contributing to the understanding of cellular biology	vascular diseases, including atherosclerosis, aneurysm and post-stent NH	progression of atherosclerosis. WSS map combined with multi-scale modelling may inform clinical practice, such as the site of rupture in aneurysm, and severity of in-stent restenosis.	WSS map. Acquisition of patient specific boundary conditions remains clinically challenging.	
Heart failure	Models based upon CT and MR help compute haemodynamics and the spatio-temporal distributions of pressure and myocardial stress/strain	CFD/FSI models replicate realistic pathophysiology in models of health and disease (eg, HFREF, HFPEF, HCM, DCM, and RWMA post-MI)	Additional haemodynamic data potentially enables early diagnosis and stratifies disease phenotypes and severities. Characterising complex vortex flows identifies areas of flow stagnation and thrombus risk	Resolution of imaging and reconstruction (representing trabeculae and papillary muscles). Tuning with realistic boundary conditions. Requirement for FSI in many models	2 34 35 36 37 38 39 40 41
CRT	Coupled electro-mechanical models of the ventricle incorporating CFD (multi-physics models) used to investigate heart function	Published reports of accurate patient-specific haemodynamic simulations with sufficient detail to optimise CRT before surgical intervention	Improved selection of CRT responders. Simulation and selection of optimal tuning of device settings and lead placement on an individual case basis	Uncertainties and assumptions regarding boundary conditions and the range of clinical measurements required for parameterisation. Mesh generation, prolonged computation times	
VADs	Generic optimisation of pump design. Patient-specific models can aid implantation strategy and tuning of output according to patient physiology	Published models describing haemodynamic influences of catheter placement and minimisation of adverse haemodynamic effects	Pump tuning to ensure periodic opening and closing of AV, preventing leaflet fusion. Personalised catheter placement planning (prediction and avoidance stasis and thrombus formation)	Post-implantation imaging artefact limits modelling. Optimising performance requires the balance of multiple competing factors. As for all cardiac electromechanical models, selection of appropriate patient specific parameters is difficult due to sparsity of data	
Congenital heart disease	CFD simulates haemodynamics which are complex and hard to predict in the context of a diverse and heterogeneous range of disease phenotypes	Range of models described, including reduced order, 3D CFD, FSI and multiscale, particularly in the context of univentricular circulation, aortic and pulmonary malformations	Modelling enables greater understanding of systemic and regional haemodynamics and the prediction of response to putative surgical or device-based treatments which often involve significant modifications to the circulatory tree	Acquisition and application of model parameters and boundary conditions from patient and literature data. The ultimate personalisation challenge	42 43 44

AV, aortic valve; CFD, computational fluid dynamics; CRT, cardiac resynchronisation therapy; CT (A), CT (angiography); DCM, dilated cardiomyopathy; FSI, fluid solid interaction; HCM, hypertrophic cardiomyopathy; HFPEF, heart failure with preserved EF; HFREF, heart failure with reduced EF; MI, myocardial infarction; NH, neointimal hyperplasia; PAP, pulmonary artery pressure; PC, phase-contrast; PCI, percutaneous coronary intervention; RA, regulatory authority; RWMA, regional wall motion abnormality; (v)FFR; (virtual) fractional flow reserve; VAD, ventricular assist device; WSS, wall shear stress.

MODEL CONSTRUCTION

CFD model construction and solution can be described in seven stages (figure 1):

1. Clinical imaging

A range of medical imaging modalities can be used, including ultrasound, CT, MRI and X-ray angiography. Imaging must provide sufficient anatomical and physiological detail, in an appropriate format and quality, to enable segmentation and data extraction.[49]

2. Segmentation and reconstruction

Segmentation methods convert medical images to in silico geometries which define the physical bounds of the model region of interest. If images are acquired over a cardiac cycle, anatomical motion can be tracked over segmented regions.[50 51]

3. Discretisation

Spatial discretisation, or 'meshing', divides the geometry into a number of discrete volumetric elements or cells. Temporal discretisation divides the solution into discrete time steps. The accuracy and numerical stability of the analysis are influenced by both spatial and temporal refinement. The fabrication of the mesh, and the level of mesh refinement, are influenced by case- and context-specific factors. The mesh and timestep (ie, spatio-temporal discretisation) must be refined enough to capture the important haemodynamic behaviour of the modelled compartment (the final solution should be independent of mesh parameters), but without excessive refinement because this impacts negatively on computational resource and solution time (see online supplementary table S1).

4. Boundary conditions

Because it is impossible to discretise the entire cardiovascular system, the region to be analysed will have at least one inlet and one outlet. To enable CFD analysis, the physiological conditions at the wall and inlet/outlet boundaries must be specified. Boundary conditions are a set of applied physiological parameters (which may vary over time) that define the physical conditions at the inlets, outlets and walls. They may be based on patient-specific data, population data, physical models or assumptions.[39]

Youtube video:

Published in heart

Computational Fluid Dynamics Modelling in Cardiovascular Medicine

Dr Paul D Morris, Dr Andrew Narracott, Professor Hendrik von Tengg-Kobligk, Dr Daniel Alejandro Silva Soto, Dr Sarah Hsiao, Dr Angela Lungu, Professor Paul Evans, Professor Neil W Bressloff, Professor Patricia V Lawford, Professor D Rodney Hose, Dr Julian P Gunn

OUTLINE

Parte IV

CFD components

Componenti della CFD

1. Modello matematico.
2. Metodo di discretizzazione.
3. Sistema di coordinate.
4. Griglia di calcolo.
5. Metodologia di approssimazione.
6. Metodo di soluzione.
7. Criterio di convergenza.

Modello matematico

- Il punto di partenza di ogni metodo numerico è, in genere, costituito dal sistema di equazioni e dalle condizioni al contorno.
- La scelta del sistema di equazioni - es. bi- o tridimensionale; incomprimibile o comprimibile; stazionario o non-stazionario etc. - è legata a:
  - Tipo di problema ed applicazione;
  - Informazioni richieste;
  - Risorse - umane, strumentali, tempo - disponibili.
- Usualmente un metodo di soluzione è stato sviluppato per un particolare set di equazioni.
- Un metodo *generale* è impraticabile (se non impossibile) e, come tutti gli strumenti general-purpose, non è mai ottimale.

Metodo di discretizzazione - 1/2

- Scelto il modello matematico, è necessario adottare il metodo di discretizzazione più conveniente o opportuno, cioè il metodo per approssimare le equazioni differenziali con un sistema di equazioni algebriche per le variabili dipendenti, definite su un insieme discreto (finito) di punti nello spazio e nel tempo;
- Esistono molti metodi, illustrati nel seguito, ma i più diffusi sono, in ordine di diffusione:
  - Volumi Finiti (FVM - *Finite Volume Method*);
  - Elementi Finiti (FEM - *Finite Element Method*);
  - Differenze Finite (FDM - *Finite Difference Method*).
- Altri metodi:
  - Elementi al Contorno (BEM - *Boundary Element Method*);
  - Metodi Spettrali (SEM - *Spectral Element Method*;
  - Metodi Lattice Boltzmann (LBM - *Lattice Boltzmann Method*);
  - Metodi Monte Carlo (DSMC - *Direct Simulation Monte Carlo* method;
  - Metodi particellari (mesh-free):
    - VMs - *Vortex Methods*;
    - SPH - *Smooth Particle hydrodynamics*.

  sono usati in CFD, ma il loro utilizzo è riservato, spesso, a classi particolari di problemi.

Metodo di discretizzazione - 2/2

- Ciascun metodo di discretizzazione fornisce la stessa soluzione se la griglia è *molto* fine.
- Tuttavia, alcuni metodi risultano più indicati per un certo problema che altri.
- La scelta del metodo è, nella realtà industriale, legata a:
  - Tipologia del problema.
  - Informazioni richieste.
  - Esperienze pregresse.
  - Competenze personali.
  - Disponibilità di software - commerciale, in-house o open source.

Sistema di coordinate

- Le equazioni di conservazione (massa, quantità di moto, energia etc.) possono venire espresse in molti modi, a seconda del sistema di coordinate e base dei vettori:
  - Cartesiano
  - cilindrico
  - sferico
  - curvilineo ortogonale
  - curvilineo non-ortogonale.
- La scelta dipende dal tipo di problema, e può influenzare il metodo di discretizzazione e la griglia utilizzata.
- Va anche scelta la base con cui definire vettori e tensori: fissa o variabile, covariante o controvariante etc.:
  - In funzione di tale scelta il vettore di velocità ed il tensore degli sforzi possono venire espressi in termini di componenti Cartesiane, covarianti o controvarianti.
- Nel seguito, se non diversamente specificato, faremo sempre uso di componenti Cartesiane.

Sistemi di coordinate curvilinee -1/3

- Un sistema di coordinate curvilinee (ξ^1, ξ^2, ξ^3) nello spazio $\mathbf{R}^3$ è definito, con riferimento ad un sistema cartesiano, da 3 funzioni del tipo:

$$\begin{cases} \xi^1 & = & \xi^1(x, y, z) \\ \xi^2 & = & \xi^2(x, y, z) \\ \xi^3 & = & \xi^3(x, y, z) \end{cases}$$

o, in notazione tensoriale:

$$\xi^j = \xi^j(x_1, x_2, x_3)$$

- La funzione vettoriale:

$$\boldsymbol{\xi} : (x_1, x_2, x_3) \rightarrow (\xi^1, \xi^2, \xi^3)$$

è definita *cambiamento di coordinate*.

- Analogamente si definisce il *cambiamento di coordinate inverso*:

$$\mathbf{r} : (\xi^1, \xi^2, \xi^3) \rightarrow (x_1, x_2, x_3)$$

- Sono definite *superfici coordinate* le superfici di equazione $\xi^j = (cost)$. Su una superficie coordinata variano solo due coordinate.
- Si chiamano *linee coordinate* le 3 linee che si ottengono intersecando a 2 a 2 le 3 superfici coordinate. Lungo tali linee varia solo una coordinata ξ^j.

Sistemi di coordinate curvilinee - 2/3

- Per un generico sistema di coordinate curvilineo ξ^j, le derivate parziali rispetto alle coordinate cartesiane possono venire espresse, dalle regole di derivazione per funzioni composte (regola della catena, o *chain rule*), in funzione delle derivate parziali rispetto alle coordinate curvilinee.
- Se A è una funzione scalare si ha

$$\frac{\partial A}{\partial x_i} = \sum_{j=1}^{3} \frac{\partial A}{\partial \xi^j} \frac{\partial \xi^j}{\partial x_i}$$

e, analogamente:

$$\frac{\partial A}{\partial \xi^i} = \sum_{j=1}^{3} \frac{\partial A}{\partial x_j} \frac{\partial x_j}{\partial \xi^i}$$

Sistemi di coordinate curvilinee - 3/3

- Ciascuna delle due formulazioni ora viste può essere usata per mettere in relazione le derivate cartesiane e curvilinee di una funzione scalare A.
- Tuttavia c'è una differenza nelle derivate della trasformazione che devono venir inserite nelle relazioni ora viste: nel primo caso è necessario valutare - o approssimare - i vettori:
$$\nabla \xi^i \quad (i = 1, 2, 3)$$
mentre il secondo richiede:
$$\mathbf{r}_{\xi^i} \quad (i = 1, 2, 3)$$
dove, ad esempio:
$$\mathbf{r}_{\xi^1} = \frac{\partial x_1}{\partial \xi^1}\mathbf{i} + \frac{\partial x_2}{\partial \xi^1}\mathbf{j} + \frac{\partial x_3}{\partial \xi^1}\mathbf{k}$$
avendo indicato per comodità con una coordinata riportata all'indice la derivazione parziale rispetto a tale coordinata.
- Perciò tutte le relazioni che riguardano la trasformazione di coordinate devono essere basate su uno o l'altro dei due set di vettori.

Base di uno spazio vettoriale

- La base di uno spazio vettoriale è un insieme di vettori linearmente indipendenti che generano lo spazio.
- In modo equivalente, ogni elemento dello spazio vettoriale può essere espresso univocamente come combinazione lineare dei vettori appartenenti alla base.
- Una base è dunque composta dal minimo numero di vettori linearmente indipendenti che genera lo spazio.
- Le *tangenti* alle linee coordinate e le *normali* alle superfici coordinate rappresentano la *base* del sistema di coordinate cuurvilinee.

Base covariante

- Si consideri una linea coordinata lungo la quale vari solo la coordinata ξ^i:

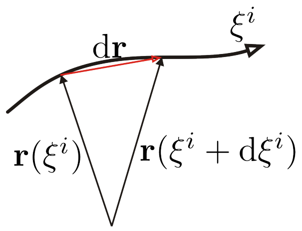

- Come noto il vettore tangente a tale linea coordinata è dato dalla:

$$\mathbf{r}_{\xi^i} = \lim_{\mathrm{d}\xi^i \to 0} \frac{\mathbf{r}(\xi^i + \mathrm{d}\xi^i) - \mathbf{r}(\xi^i)}{\mathrm{d}\xi^i}$$

- Questi 3 vettori tangenti alle tre linee coordinate costituiscono la base vettoriale *covariante* del sistema di coordinate curvilinee, e sono indicati con:

$$\mathbf{a}_i = \mathbf{r}_{\xi^i} \quad (i = 1, 2, 3)$$

dove, come già visto, le tre coordinate curvilinee sono indicate con ξ^i, $(i = 1, 2, 3)$, e il pedice i indica il vettore base relativo alla coordinata ξ^i, vale a dire il vettore tangente alla linea coordinata lungo la quale varia solo ξ^i.

Base contravariante

- Un vettore normale ad una superficie coordinata sulla quale la coordinata ξ^i è costante è dato da $\nabla\xi^i$:

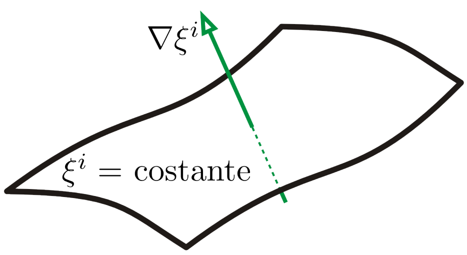

- Questi 3 vettori normali alle tre superfici coordinate costituiscono la base vettoriale *contravariante* del sistema di coordinate curvilinee, e sono indicati con:

$$\mathbf{a}^i = \nabla\xi^i \quad (i = 1, 2, 3)$$

- In questo caso l'indice i è indicato come apice sui vettori della base *contravariante*, al fine di distinguerli dalla base vettoriale *covariante*.

Base covariante e controvariante

- La seguente figura, nella quale è riportato un elemento di volume a sei lati, ciascuno dei quali giace su una superficie coordinata, illustra i due tipi di base:

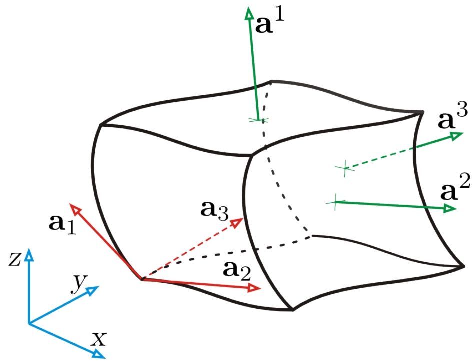

- Nella figura seguente è riportata la scomposizione di un generico vettore $\mathbf{v}$, per semplicità nel piano, nelle componenti *cartesiane* $\mathbf{v}_i$, nelle componenti *covarianti* $\mathbf{u}_i$ e nelle componenti *controvarianti* $\mathbf{u}^i$:

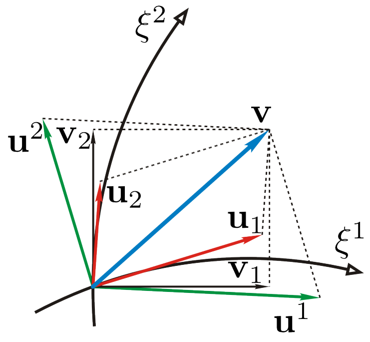

Sistemi di coordinate curvilinee ortogonali

- Solo in un sistema di coordinate curvilinee *ortogonali* i vettori base dei due sistemi - covariante e controvariante - sono paralleli, poichè per uin sistema di coordinate curvilinee *non ortogonale* la normale ad una superficie coordinata non coincide necessariamente con la tangente alla linea coordinata che attraversa tale superficie:

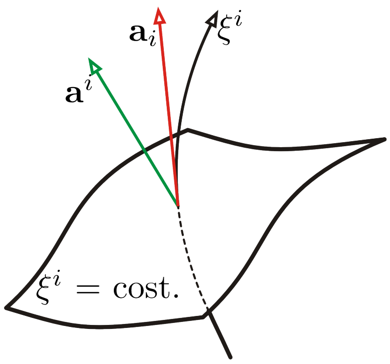

- In un sistema di coordinate curvilinee ortogonali i tre vettori base, di ciascun tipo, sono mutuamente ortogonali.

Griglia di calcolo - 1/5

- I punti (finiti) nei quali calcolare le variabili sono definiti dalla griglia (*grid* o *mesh*), che rappresenta in modo discreto il dominio geometrico nel quale il problema va risolto.
- Le tipologie di griglie più diffuse sono:
  1. Strutturate (Cartesiane, ortogonali e non-ortogonali)
  2. Strutturate a blocchi
  3. Non strutturate.

Griglia di calcolo - 2/5

Esempio di griglia strutturata 2D attorno ad un profilo alare NACA 0012

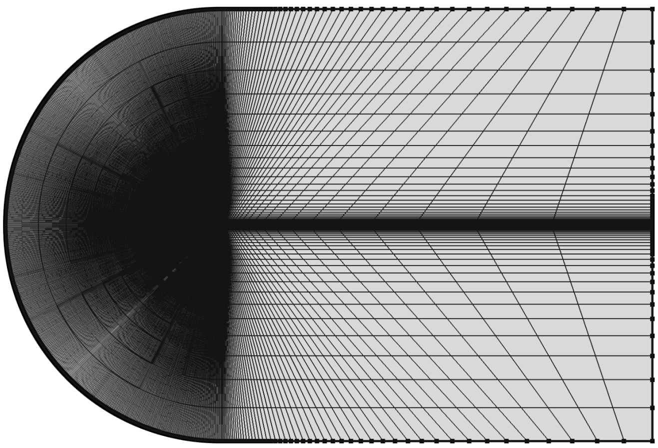

Vista complessiva

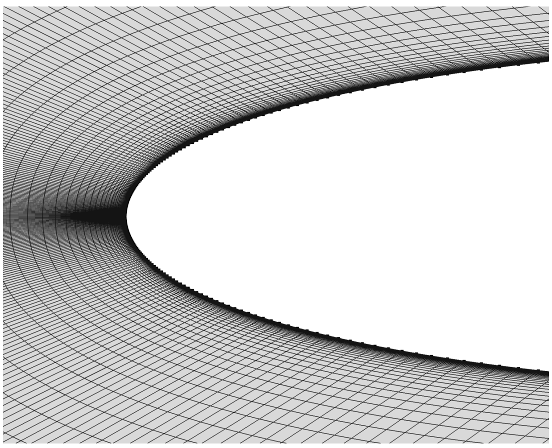

Dettaglio sul bordo d'ingresso

Griglia di calcolo - 3/5

Esempio di griglia strutturata tipo *overset* (chimera)

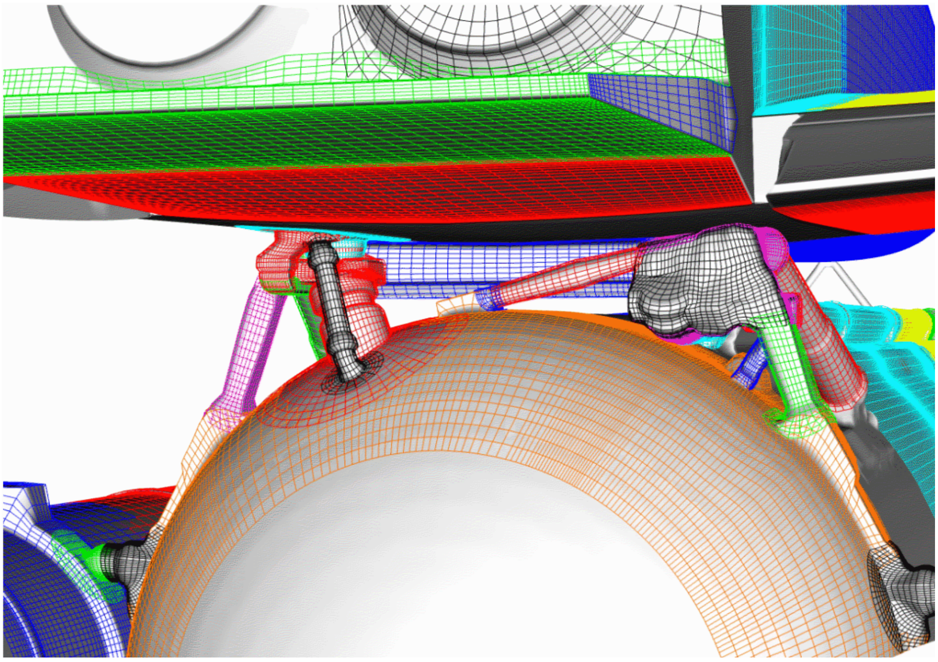

Griglia di calcolo - 4/5

Example of an unstructured surface grid

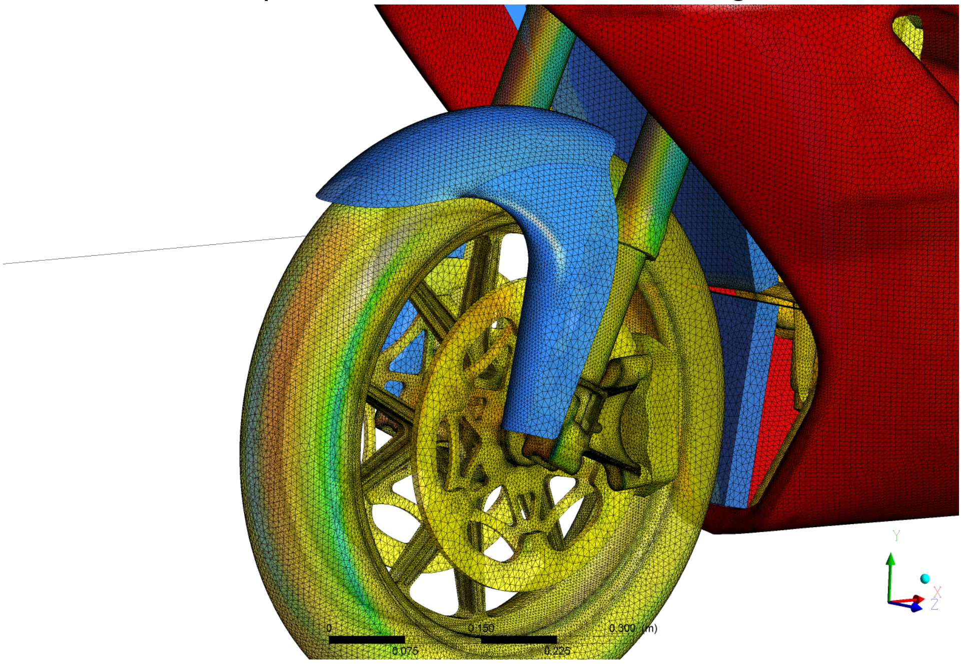

Griglia di calcolo - 5/5

Examples of (a) trimmed mesh and (b) polyhedral mesh.

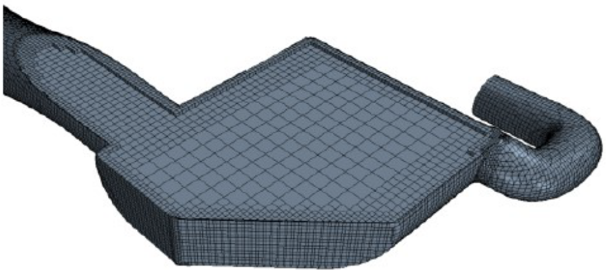

(a)

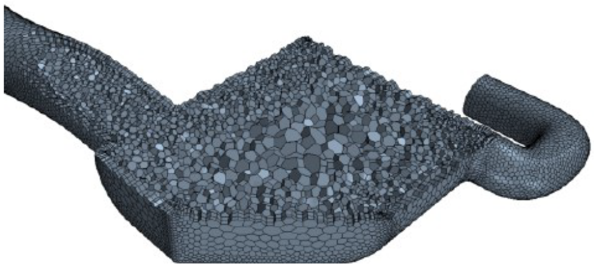

(b)

- Dopo aver scelto la tipologia di griglia, è necessario scegliere la/le approssimazione/i usata/e nella discretizzazione:
  - In FDM, vanno scelte le approssimazioni per le derivate nei punti della griglia
  - In FVM vanno selezionati i metodi di interpolazione (per valutare i valori delle variabili in punti diversi dai nodi della griglia), ed i metodi per approssimare integrali di superficie e di volume
  - In FEM vanno scelte le funzioni di forma (elementi) e le funzioni peso
- Esistono molte possibilità di scelta, con importanti conseguenze sull'accuratezza della soluzione;
- I metodi del 2^o ordine rappresentano spesso un buon compromesso fra accuratezza, semplicità ed efficienza computazionale.

Metodo di soluzione - 1/2

- La discretizzazione produce - usualmente - sistemi algebrici di equazioni di rilevante dimensione:
  - Tali sistemi possono essere lineari (es. metodi espliciti o semi-impliciti) o, più frequente per le applicazioni industriali, non-lineari. Questi ultimi vanno poi opportunamente linearizzati prima di procedere alla loro soluzione.
- Per problemi non stazionari, si utilizzano spesso metodi *simili* a quelli usati per problemi, ai valori iniziali, descritti da equazioni differenziali ordinarie: time-marching:
  - In generale, almeno per flussi incomprimibili, è necessario risolvere un problema *ellittico* ad ogni passo di tempo.
- I problemi stazionari vengono affrontati - come si vedrà - ricorrendo ad una sorta di avanzamento temporale: *pseudo-time marching*, o analogo schema iterativo.

Metodo di soluzione - 2/2

- Poiché, come già detto, le equazioni sono non-lineari, esse vanno risolte *iterativamente*, usando un opportuno sistema di linearizzazione - *OUTER ITERATIONS*:
  - Tali *iterazioni esterne*, inoltre, sono sempre necessarie qualora vi siano equazioni accoppiate in modo non-lineare (es. modelli di turbolenza)
  - Le *iterazioni esterne* possono venire interpretate come passi *distorti* di integrazione temporale, e la soluzione del problema stazionario corrisponde alla soluzione asintotica, per $\tau \to \infty$, dell'analogo problema non stazionario.
- I sistemi lineari così ottenuti sono, in genere, di grande dimensione e sono usualmente risolti, nella pratica industriale, attraverso tecniche iterative - *INNER ITERATIONS*;
- La scelta dell'algoritmo di risoluzione del sistema di equazioni lineari - ottenuto dalla linearizzazione - dipende da:
  - Tipo di griglia
  - Numero di nodi/celle
  - Tipo di equazione (correzione di pressione, quantità di moto, energia cinetica turbolenta etc.).

Criteri di convergenza

- Utilizzando metodi iterativi, è necessario stabilire i *criteri di convergenza*, cioè definire i valori limite di alcune grandezze - indicatori di convergenza - oltre i quali è inutile, e/o dispendioso, proseguire con le iterazioni:
  - Outer iterations: necessarie a causa della non-linearità ed accoppiamento delle equazioni;
  - Inner iterations: usate per risolvere i sistemi lineari di equazioni.

OUTLINE

Parte V

CFD workflow

Classical CFD workflow

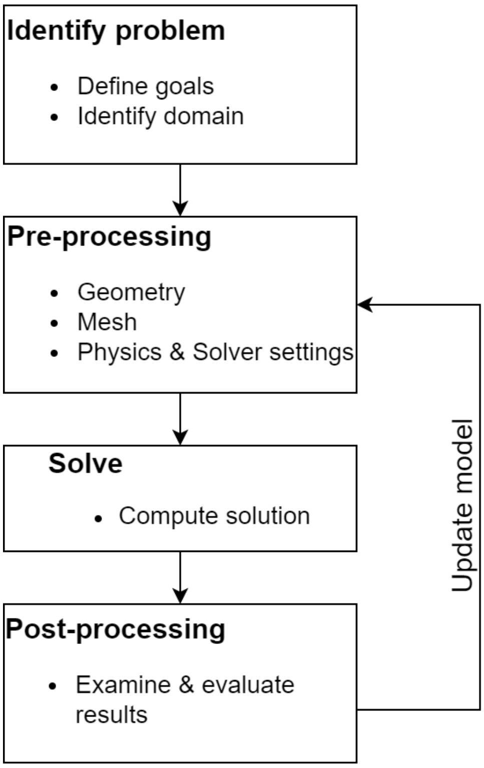

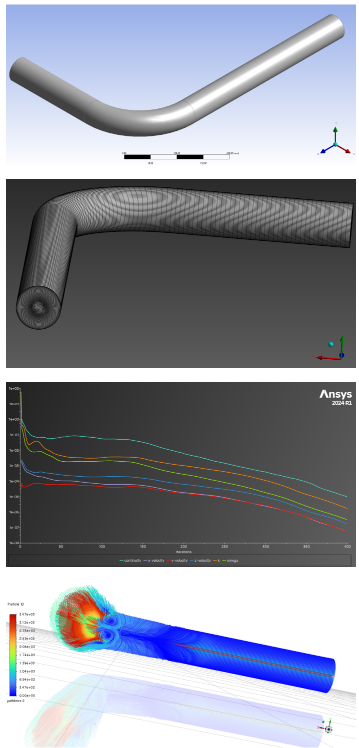

Modeling goals

- What results are required, e.g. pressure drop, mass flow rate, heat flux, lift force et.
- What modeling options and semplifications are deem acceptable?
  - What simplifying assumptions can/must be made, e.g. steady-state, 2D, symmetry, periodicity, et.
  - What physical models must be included in the analysis (turbulence, heat transfer, free surface et.)
- What degree of accuracy is required ?
- How many resources (time, computing platforms, man-hours) are available?
- Is CFD an *appropriate* tool at this stage?

Choice of Domain and mesh resolution

- How you select the part/component of the system to analyze?
- Are boundary conditions available?
- Can it be approximated as e.g. 2D or axi-symmetric ?
- How will you obtain a model of the *fluid* region?
  - Use an existing CAD model?
  - Extract the *fluid* region from a solid part?
  - Create from scratch?

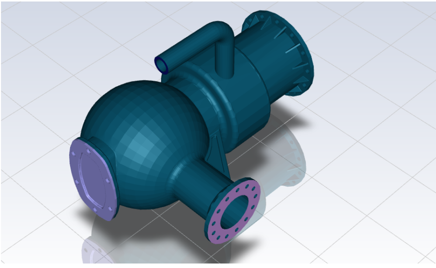
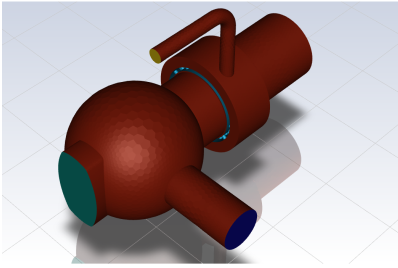
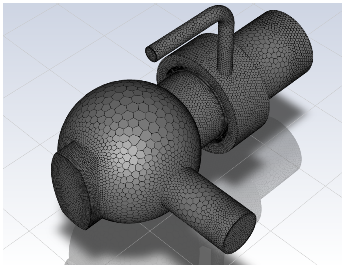

- What is the required mesh resolution?
- Are adequate computational resources available?

Computing the solution

- The discrete equations are solved iteratively until convergence
- Convergence is reached when:
  - Residuals are below a specified tolerance, *e.g.* 1×10^{-5}
  - Overall conservation is achieved, e.g. mass flow in = mass flow out
  - Quantities of interest - lift, drag. heat flux, force et. - do not change anymore
- The accuracy of a solution is dependent upon:
  - Degree of convergence
  - Mesh independence
  - Appropriateness of mathematical (physical) model

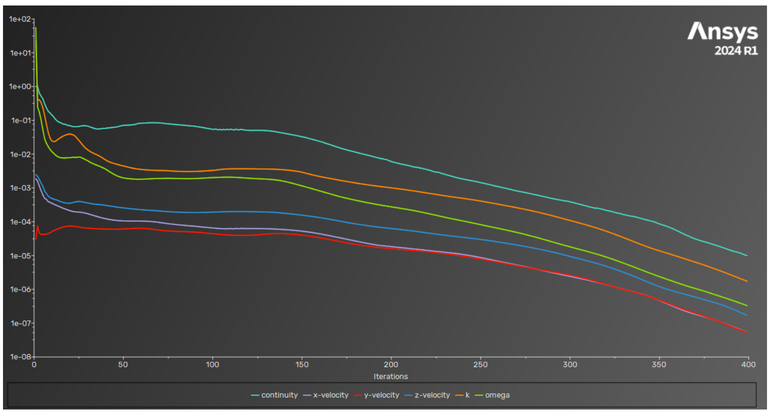

Examine the results and review the model

- Examine the results:
  - What is the overall flow pattern?
  - Is there separation/reattachment?
  - Is the heat flux uniformly distributed?
  - Are the most important flow features adequately resolved?

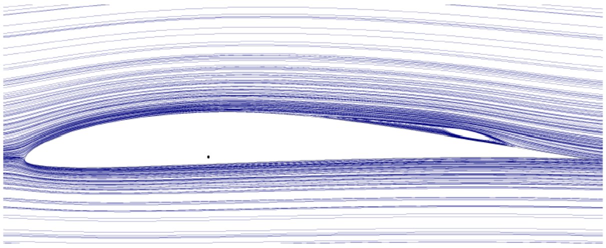

- Evaluate quantitative results:
  - Flow rate, pressure drop
  - Forces (drag, lift), moments
  - Average heat transfer coefficients
  - Highest temperature
  - Surface/volume integrated/averaged quantities
- Are the physical models appropriate. e.g. laminar/turbulent, steady/unsteady et.
- Is the computational domain adequate?
- Are boundary conditions correct?
- Is the mesh adequate, *e.g* does the model contains (some) poor quality cells?

OUTLINE

Parte VI

Numerical Methods in CFD

Consistenza

- La discretizzazione dovrebbe fornire il valore *esatto* quando la dimensione della griglia - spaziale e temporale - tende a zero.
- La differenza fra l'equazione discretizzata e quella esatta è chiamata *errore di troncamento*:
    - Stimato sostituendo i valori nodali nell'approssimazione discreta con un'espansione in serie di Taylor (si vedranno alcuni esempi parlando di *Differenze Finite*);
    - Il risultato è l'equazione differenziale originaria più un *resto*, che rappresenta l'errore di troncamento.
- Affinché un metodo possa definirsi *consistente*, l'errore di troncamento deve diventare nullo quando la dimensione della griglia tende a zero: $\Delta x_i \to 0$ e $\Delta \vartheta \to 0$.
- L'errore di troncamento è usualmente proporzionale ad una potenza di Δx_i e/o $\Delta \vartheta$:
    - ➢ Δx_i^n Metodo di ordine n ($n > 0$) nello spazio (accuratezza spaziale dell'n-esimo ordine);
    - ➢ $\Delta \vartheta^m$ Metodo di ordine m ($m > 0$) nel tempo (accuratezza temporale dell'm-esimo ordine).
- Idealmente, tutti i termini dell'equazione dovrebbero venire discretizzati con approssimazioni dello stesso ordine, ma in qualche caso è preferibile trattare in modo più accurato i termini dominanti (es. termini convettivi per flussi ad elevato numero di Reynolds).
- Anche se l'approssimazione è consistente, ciò non garantisce, in generale, che la soluzione dell'equazione discretizzata diventerà uguale a quella esatta per $\Delta x_i \to 0$: il metodo di soluzione dev'essere *stabile*.

Stabilità

- In modo semplice, possiamo definire *Stabile* un metodo di soluzione numerica che *non amplifica* gli errori che (inevitabilmente) appaiono nel corso della soluzione:
    - Per i metodi iterativi, un *metodo stabile* è un metodo che *non diverge*;
    - Per i problemi non stazionari, la stabilità garantisce che il metodo fornisca una soluzione *bounded* quando la soluzione esatta dell'equazione è *bounded*.
- La stabilità è difficile da quantificare, in particolare per problemi non-lineari con condizioni al contorno realistiche:
    - Approccio semplificato: problemi lineari a coefficienti costanti in assenza di condizioni al contorno.
- L'approccio più utilizzato, nello studio della stabilità, è il metodo di *Von Neumann*;
- Nell'affrontare problemi complessi, tipici dell'ambito industriale, con equazioni non-lineari accoppiate e complesse condizioni al contorno, non è facile stabilire i criteri di stabilità:
    - Limite sul passo di tempo (anche per metodi puramente impliciti);
    - Necessità di sotto-rilassamento;
    - ...
    - Esperienza ed intuizione !

Convergenza

- Un metodo numerico è definito convergente se la soluzione delle equazioni discretizzate *tende* alla soluzione esatta (dell'equazione differenziale) quando $\Delta x_i \to 0$;
- Convergenza *non* è sinonimo di consistenza;
- Per problemi lineari ai valori iniziali, il *teorema di equivalenza di Lax* (Richtmyer and Morton, 1967), stabilisce che:

Teorema

Per un problema lineare ai valori iniziali ben posto ed una sua approssimazione alle differenze finite che soddisfa la condizione di consistenza, questa è convergente se e solo se essa è stabile.

- Un metodo consistente, ma non stabile, *non* è convergente e, come tale, è inutile;
- Nella pratica, la convergenza viene determinata sulla base di esperimenti numerici su griglie via via più fini:
  - Soluzione *grid-independent*;
  - Per griglie *sufficientemente fini*, il grado di convergenza è determinato dall'ordine di troncamento;
  - Stima dell'errore nella soluzione.

Conservazione

- Le equazioni da risolvere sono *equazioni di conservazione* (v. *Introduzione alle leggi del moto dei fluidi*), perciò i metodi numerici utilizzati dovrebbero rispettare - globalmente e localmente - tali leggi:
  - In condizioni stazionarie e senza sorgenti, l'ammontare di una quantità, ad esempio la massa, che esce da un volume chiuso, dev'essere pari alla quantità in entrata.
- Utilizzando le equazioni nella forma conservativa (divergenza), ed adottando il metodo dei *Volumi Finiti*, la conservazione è garantita su base locale (Volume Finito) e globale (intero dominio);
- Anche gli altri metodi, ad esempio il metodo degli *Elementi Finiti*, possono venire resi conservativi;
- Il trattamento dei termini sorgenti dev'essere consistente, in modo che la quantità totale di una quantità generata (sorgente) o assorbita (pozzo) nel dominio sia pari al flusso netto della stessa quantità attraverso il contorno del dominio stesso;
- La conservazione è una proprietà fondamentale, poiché impone un vincolo/limite all'errore della soluzione.

Limitazione (boundedness) e realizzabilità (realizability)

Limitazione (boundedness)

- Le soluzioni numeriche dovrebbero rimanere all'interno di opportuni limiti:
  - Quantità non-negative – es. densità, energia cinetica turbolenta – dovrebbero sempre rimanere positive, possibilmente anche durante le iterazioni intermedie;
  - Quantità, come concentrazioni, dovrebbero essere comprese fra 0 e 1 (0% - 100%);
  - In assenza di sorgenti, le temperature devono essere comprese fra quelle dei contorni.

Realizzabilità (realizability)

- I modelli di fenomeni troppo complessi da venire affrontati direttamente, es. turbolenza, combustione, flussi multifase etc., devono dar luogo a soluzioni fisicamente realistiche.

Accuratezza - 1/2

- Le metodologie della fluidodinamica numerica danno sempre luogo a *soluzioni approssimate*;
- A parte eventuali errori introdotti nella fase di *set-up* (errori di programmazione (bugs), scelta errata dell'algoritmo di soluzione, condizioni al contorno incorrette etc.), la soluzione è sempre affetta da *tre tipi di errori sistematici*:

Errori di modellazione: differenza fra il *problema reale* e la *soluzione esatta del modello matematico*. Si tratta di errori dovuti, a titolo di esempio, alle ipotesi alla base del problema (stazionarietà o meno; 2D o 3D; eventuale periodicità etc.), alla scelta del dominio di calcolo, alla scelta del modello di turbolenza, alle condizioni al contorno, alla limitata conoscenza delle proprietà termofische, alla scelta di eventuali modelli multifase, alla scelta del modello di combustione etc.;

Errori di discretizzazione: differenza fra la *soluzione esatta delle equazioni (modello matematico)* e la *soluzione esatta dei sistemi di equazioni* ottenuti con la discretizzazione. Esso si riduce all'aumentare dell'infittimento della griglia;

Errori di convergenza: differenza fra la *soluzione esatta dei sistemi di equazioni* e la *soluzione ottenuta attraverso algoritmi iterativi*. Esso si riduce all'aumentare del numero di iterazioni.

Accuratezza - 2/2

- È particolarmente importante tenere in conto tali errori, e soprattutto saperli distinguere;
- Alcuni errori possono risultare dominanti, e talvolta assumono valore uguale e segno opposto, con la conseguenza di dar luogo, ad esempio, a accuratezza maggiore di simulazioni effettuate su griglie più rade;
- Per poter stabilire gli eventuali errori di modellazione, è dapprima necessario verificare compiutamente gli errori di convergenza e di discretizzazione;
- Esistono vari modi per affrontare numericamente un problema di termofluidodinamica, ma è importante ricordare che, nelle applicazioni, l'obiettivo è spesso quello di ottenere l'accuratezza desiderata con il minimo sforzo, oppure - più frequente - la massima accuratezza con le risorse disponibili.